Relationship Between Intermolecular Bonding, Nanostructure, Phase Behavior, and Macroscopic Physical Properties of Pressure-Sensitive Adhesives Based on Polyelectrolyte Complexes

T. I. Levada (Kiseleva),[1] M. M. Feldstein[2,3]

[1]*A.V. Topchiev Institute of Petrochemical Synthesis, Russian Academy of Sciences, Moscow, Russia*
[2]*A.N. Nesmeyanov Institute of Organoelement Compounds, Russian Academy of Sciences, Moscow, Russia*
[3]*D.I. Mendeleyev Russian University of Chemical Technology of Russia, Moscow, Russia*

Received 24 June 2011; accepted 13 September 2011
DOI 10.1002/app.35649
Published online 20 December 2011 in Wiley Online Library (wileyonlinelibrary.com).

ABSTRACT: Correlations have been established between mechanisms of molecular interaction, the energy of intermolecular bonds, nanoscopic free volume, phase state, and such macroscopic physical properties as linear and large-strain viscoelasticity, relaxation, water-absorbing capacity, and adhesive joint strength of pressure sensitive adhesives based on nonstoichiometric polyelectrolyte complexes. The polyelectrolyte complexes are formed by mixing of a polybase, copolymer of *N,N*-dimethylaminoethyl methacrylate with methyl methacrylate and butyl methacrylate (PDMAEMA-*co*-MMA/BMA), with a polyacid, copolymer of methacrylic acid and ethyl acrylate (PMAA-*co*-EA) in the presence of triethyl citrate (TEC) as a plasticizer. Rubber-like elasticity and pressure sensitive adhesion of the polyelectrolyte complexes on the macroscopic level have been demonstrated to be the result of specific coupling of such generally conflicting properties of polymer materials as sufficiently strong intermolecular cohesion energy with comparatively large free volume (vacant space between neighboring macromolecules) at the nanoscopic scale.
 J Appl Polym Sci 125: 448–470, 2012

Key words: polyelectrolyte complexes; nanostructure; intermolecular cohesion and free volume; phase state; viscoelasticity; relaxation and pressure sensitive adhesion

INTRODUCTION

Phase state and physical properties of polymer materials relate to their chemical structure.[1–3] If a quantitative structure–property relationship (QSPR) is explored, a number of fundamental physical characteristics of polymers may be predicted from their chemical structure.[4,5] Numerous correlations have been reported in literature between chemical structures of polymers,[6–8] mechanisms of their molecular interactions in blends[9] on the one hand, and the phase state of polymer composites on the other. In turn, on a macroscopic scale the physical properties of polymer materials are governed by their phase state and, consequently, by the molecular structure.[10–15] In particular, the examination of the relationship between rheological properties of polymers and their molecular structure is the subject of a longstanding interest. During the past two decades, the comprehension of this relationship has been considerably improved, particularly owing to the development of molecular-dynamics theories.[16,17] Theoretical models relating molecular structures and dynamics to the macroscopic viscoelastic behavior of polymers are of obvious academic interest. On the other hand, careful experimental characterization of the structure-viscoelasticity relationship is highly important for the industry of polymer materials. Actually, processing of polymer materials as well as their end-use performance properties are directly governed by their rheological behavior. By this means, bridging a gap separating molecular and nanostructures of polymer materials with their macroscopic performance properties is a problem of greatest fundamental and practical significance. In its turn, a pathway from nanostructure toward macroscopic properties of polymers passes through their phase behavior and their microscopic physical properties.

While correlations between viscoelastic properties and molecular structure of polymers is relatively well explored and described in literature,[18] there is a lack in fundamental knowledge on similar relationships linking molecular structures to pressure sensitive adhesion of polymer composites.[19,20]

Correspondence to: M. M. Feldstein (mfeld@ineos.ac.ru or feldhome@gmail.com).
Contract grant sponsor: Russian Ministry of Education and Science; contract grant number: 16.513.11.3048.

From practical point of view, knowledge of the QSPR is also of considerable importance for rational design of new materials with tailored performance properties. The final goal of our research is an innovative molecular design method for rational development of new pressure-sensitive adhesives (PSA) with tailored performance properties, which can be produced by blending of nonadhesive hydrophilic functional polymers. The PSA are viscoelastic polymer materials capable of forming strong adhesive bonds with substrates of various chemical nature under application of a slight pressure (1–10 Pa) over a short contact period (1–2 s).[21]

To establish polymer molecular structures responsible for pressure sensitive adhesion, in our recent research[22] we employed the relationships between adhesion and viscoelastic behavior of the PSAs, which have been a subject of numerous investigations.[20,23,24]

General characteristic feature of all the PSAs is that they demonstrate large tensile deformations and fibrillation of adhesive layer during debonding process in the course of peel[22,25] or probe tack tests.[26–28] These fibrils elongate up to a few hundred and even thousands of percentages compared with the thickness of intact adhesive layer. In this sense it is of no wonder that direct relationship occurs between 180° peel force (***P***) and uniaxial tensile stress–strain behavior of the PSAs, which is described by eq. (1):

$$P = k \cdot b \cdot l \cdot \int_0^{\varepsilon_b} \sigma \cdot d\varepsilon \tag{1}$$

where ***b*** and ***l*** are the width and thickness of the adhesive film, σ and ε are the tensile stress and relative elongation, ε_b is the maximum elongation of the film at the break, and k is a constant that takes into account the contributions of backing film deformation and interfacial interaction between the adhesive and the substrate. If we compare the peel adhesion of various adhesives using the same backing film and a standard high-energy substrate, we can accept $k \approx 1$. Assuming further that the deformation of the adhesive film in the course of both debonding and uniaxial drawing follows the linear elastic law, the eq. (1) can be written as:

$$P = \frac{b \cdot l \cdot \sigma_b^2}{E} \tag{2}$$

where the σ_b is the ultimate tensile strength and E is an approximate tensile modulus of the adhesive material. For the PSAs this is not a bad approximation because they usually soften and then harden at large strains. The eq. (2) is similar to the well-known Kaelble equation[29]:

$$P = \frac{b \cdot l \cdot \sigma_f^2}{4E} \tag{3}$$

where σ_f is a critical value of ultimate stress at a fracture of PSA material under debonding from a substrate with a fixed rate. The implication of the similarity of eqs. (2) and (3) is that the Kaelble eq. (3) holds for any types of pressure sensitive adhesives. Thus, the rule described by eqs. (2) and (3) is universal.

The eq. (2) relates adhesion to macroscopic large-strain tensile properties of polymer materials. However, this equation can be easily modified to express the peel adhesion (P), as an explicit function of the relaxation time (τ) and the self-diffusion coefficient (D) of a PSA polymer chain segment. Indeed, let us assume in the first approximation that a PSA represents a viscoelastic material that can be described with a Maxwell model characterized with a single apparent relaxation time (τ) and a microviscosity (or monomer–monomer friction coefficient of polymer chain), η. Taking into account that according to the Maxwell model $E = 3\eta/\tau$, we obtain:

$$P = b \cdot l \frac{\tau}{3\eta} \sigma_b^2 \tag{4}$$

The viscosity of the Maxwell model can then be substituted by the classical Einstein expression[30]:

$$\eta = \frac{kT}{DaN} \tag{5}$$

where N is a number of monomer units of size a in a segment of polymer chain and D is the self-diffusion coefficient of polymer segment. Substitution of obtained values into the eq. (4) yields the eq. (6) that relates adhesion to the microscopic (molecular dynamic) properties of polymers:

$$P = b \cdot l \cdot \frac{a \cdot D \cdot \tau}{3kT} \cdot \sigma_b^2 \tag{6}$$

where a represents now the size of polymer chain segment, k is the Boltzmann constant, and T is temperature.

Equation (6) is, of course, only qualitatively illustrative, because it makes many crude approximations including ignoring the existence of the spectrum of relaxation times. It is inappropriate for quantitative calculations of peel force, because it includes immeasurable terms like a (the size of the diffusing polymer segment). Nevertheless, it predicts qualitatively the significance of diffusion and relaxation processes (both of which require molecular mobility) for the adhesive behavior of polymers when their debonding is dominated by the formation of

fibrils. Equation (6) was derived on the basis of the analysis of the deformation contribution to peel adhesion without resorting to the so-called diffusion theory of adhesion, earlier offered by Voyutskii.[31] Thereby, the rheological approach based on the analysis of viscoelastic deformation of the adhesive material under debonding process, has more universal character than others mechanisms of adhesion, considered in Ref. [19].

According to the eq. (6), pressure sensitive adhesion requires a coupling of high molecular mobility, embedded by the high value of the self-diffusion coefficient of adhesive polymer segment (D), with long-term relaxation processes outlined by large values of the relaxation time (τ), and a high cohesive strength of adhesive polymer, expressed in the terms of ultimate tensile stress at the break of the stretched adhesive under uniaxial drawing (σ_b).

On a nanoscopic scale, high molecular mobility is a manifestation of large free volume. A fundamental quantity that underlies a high value of the self-diffusion coefficient at molecular level is a fraction of free volume (f_v)[32]:

$$D = A \cdot \exp\left(-B/f_v\right) \tag{7}$$

where A and B are constants. The free volume is defined as the unoccupied space, or vacancies, available for segmental motion and diffusion of polymer chains. In such a manner, the eq. (6) bridges the gap between macroscopic adhesive properties and nanostructure of polymer materials.

A specific feature of all pressure sensitive adhesives is that they should combine a high energy of cohesive interaction with a large free volume. Most commonly, strong cohesive interaction between macromolecules causes a drastic decrease in the free volume, which explains why the pressure sensitive adhesion is comparatively rare phenomenon.

Although both the diffusion coefficient and the relaxation time are the measures of molecular mobility, they do vary in opposite directions under the transition from glassy polymer to viscous liquid. Indeed, the longest relaxation times are featured for glasses, whereas low-molecular-weight liquids relax almost instantaneously. In contrast, the lowest diffusion coefficients are observed for glasses, whereas the highest diffusion coefficients are observed in liquids and gases. According to eq. (6), maximum peel strength (P), relates to the maximum magnitude of the ($\tau \cdot D \cdot \sigma_b$) product. Evidently, this product achieves its maximum magnitude in a certain range of values of relaxation time and diffusion coefficient, which are intermediate between those inherent for liquids and glasses. The materials coupling the properties of the liquids and the solids are in a viscoelastic state, which is why all PSAs are viscoelastic materials.

A question arises: What magnitudes of diffusion coefficient (D), relaxation time (τ), and ultimate tensile strength under uniaxial drawing of adhesive films (σ_b) are in favor of high adhesion? In the series of our recent publications we have already considered the significance of high diffusivity[22] and longer relaxation times[33–36] for high adhesion.

In accordance with eqs. (6) and (7), pressure sensitive adhesion is the result of specific balance between high energy of intermolecular cohesion and large free volume. Hence, to develop PSA rationally we should identify the molecular structures that meet these usually conflicting requirements.

As recent investigations in our group have shown, mechanisms of formation of interpolymer and polymer–oligomer complexes can underlie the molecular design of new pressure-sensitive adhesives prepared by blending of nonadhesive polymers and oligomers bearing complementary functional groups at both ends of their short chains.[37–39] Mechanisms of molecular interactions as well as energetic and geometric characteristics of hydrogen bonds providing the formation of polymer–oligomer complexes were the subject of our recent research.[40] In next article of this series we examined the effects of intermolecular bonding on the phase state, mechanical properties and adhesion of the PSAs based on the polymer–oligomer complexes.[41] At last, in the most recent article we analyzed the effects of intermolecular hydrogen bonding and nanostructure on mechanical and adhesive properties of the polymer–oligomer complexes.[42]

In polymer blends involving the formation of polyelectrolyte complex between macromolecules of a polybase and a polyacid, high cohesion strength is provided by hydrogen, electrostatic, or ionic bonding between macromolecules carrying complementary reactive groups in recurring units of their main chains, whereas large free volume can result from the occurrence of loops and other defects of supramolecular network structure. Although a considerable amount of research work has been performed on the investigation of formation mechanisms and properties of interpolymer and polyelectrolyte complexes in solutions,[43–53] there is a lack of experimental data on the phase behavior of oppositely charged polyelectrolyte blends in a solid state. Relationship between mechanisms of molecular interactions in the binary and ternary blends of polybase and polyacid with and without appropriate plasticizer, and the phase state of polyelectrolyte blends involving nonstoichiometric and stoichiometric polybase–polyacid complex formation have been considered in details in two recent papers of our group.[54,55] Nanostructure and free volume in the PSAs based on the

nonstoichiometric polyelectrolyte complex are also examined.[56] In the present and concluding article of this series we attempt to bridge a gap between nanostructure, phase state and macroscopic, adhesive and mechanical properties of PSAs based on solid-state nonstoichiometric polyelectrolyte complexes, and gain a molecular insight into adhesion and viscoelastic behavior of these innovative PSAs. With this purpose, here we first summarize the most important results of our earlier studies of intermolecular cohesion energies,[54] nanostructure,[56] and phase state[55] of the PSAs formed in plasticized polybase–polyacid blends. In order to establish the values of intermolecular cohesion energy, the size and relative fraction of the free volume, favoring good adhesion, we then compare these data to adhesion, linear viscoelasticity, and large-strain tensile properties of the polyelectrolyte complexes.

EXPERIMENTAL

Materials

As a polybase in this work we used the copolymer of *N,N*-dimethylaminoethyl methacrylate (DMAEMA) with methyl methacrylate (MMA) and butyl methacrylate (BMA) (PDMAEMA-*co*-MMA/BMA), molar ratio = 2 : 1 : 1, molecular weight ~ 150,000 g/mol. The polybase is commercially available from Röhm Pharma GmbH (Darmstadt, Germany) as Eudragit® E-100. As a polyacid, we employed a copolymer of methacrylic acid (MAA) with ethyl acrylate (EA) (PMAA-*co*-EA), molar ratio = 1 : 1, molecular weight ~ 250,000 g/mol, which was obtained as Eudragit® L-100-55 from Evonik Degussa Corp. (Piscataway, NJ), subsidiary of Evonik Röhm GmbH, (Germany). Another polyacid used in present research was a copolymer of maleic acid with methylvinyl ether (PMA-co-MVE), molar ratio = 1 : 1, molecular weight ~ 1,980,000 g/mol, obtained as Gantrez S-97 BF from ISP Corporation (Wayne, NJ). All the polymers were used as received. Tackifier Regalite R9110 (glycerol ester of tall oil rosin) was obtained from Hercules (Wilmington, DE).

Preparation of polyelectrolytes charged to a predetermined degree of ionization of ionogenic groups was provided by the treatment of their water–alcohol (50 : 50) solutions by aqueous solutions of HCl (for polybase ionization) or NaOH (for ionization of polyacid). With this purpose the amounts of HCl or NaOH required for full ionization of the ionogenic groups was measured in advance by means of potentiometric titration. The degrees of polyelectrolyte ionization of 10 and 50% corresponded to 0.1 and 0.5, respectively, of the gram equivalents of the HCl and NaOH required for full ionization of the polyelectrolyte.

According to potentiometric titration data, the initial PDMAEMA-*co*-MMA/BMA copolymer contained no protonated aminogroups. At the same time, the degree of dissociation of the carboxyl groups in initial PMAA-*co*-EA polyacid was 2.5–3%.

Plasticizers, employed in this work, were triethyl citrate (TEC), tributyl citrate (TBC), acetyltriethyl citrate (ATEC) and acetyltributyl citrate (ATBC), obtained from Morflex (Greensboro, NC).

Preparation of experimental samples

The films of polybase–polyacid blends with and without plasticizer were prepared by casting-drying method from ethanol solutions. Required amount of polybase was first dissolved in ethanol under vigorous stirring (600–700 rpm) using a Cole-Parmer (Vernon Hill, IL) laboratory mixer (model 50002-25). Stirring rate was then increased to 900–1000 rpm and the PMAA-*co*-EA polyacid was slowly step-by-step added. This mixture was then kept stirred for 16 h until a homogeneous solution was obtained. TEC plasticizer was added to the polymer solution under stirring on a magnetic stirrer. The total concentration of polymers in ethanol averaged 38–40 wt %. Solutions containing 20 : 1 and 10 : 1 polybase–polyacid weight ratios were clear. Then they were cast onto a poly(ethylene terephthalate) casting sheet (PEBAX-600 from Arkema Inc., Philadelphia, PA). A uniform thickness of the films was obtained by using the BYK-Gardner film casting knife (AG-4300 Series, Columbia, MD) as described earlier.[57] The wet film thickness was 0.5 mm and the thickness of dry film was 80–100 μm. The films were dried overnight at ambient conditions (19–22°C). Upon drying, the films were covered by the second sheet of the release liner.

For Probe Tack adhesion measurements, all the PSA films of 100–110 μm in thickness were prepared by casting their solutions onto glass slide previously cleaned with ethyl alcohol, followed by drying at 60°C until constant weight was achieved (24–36 h).

For DMA measurements the unsupported PSA films were prepared by casting the solutions onto the Loparex PET siliconized release liner (Eden, NC) of 50 μm in thickness.

Research methods

FTIR spectra

FTIR spectra of the films from the blends and parent components were recorded within the range of wavelengths 4000–400 cm^{-1} using Bruker IFS-113v and IFS-66 v/s spectrometers (Ettlingen, Germany) with a resolution of 1 cm^{-1} as earlier described.[54] Four hundred scans were done for each spectrum. Films used as specimens were cast on Si plates from

15 to 20% ethanol solutions followed by drying for 24 h at ambient temperature. The thickness of dry films was 10–15 μm. The spectra were treated using GRAMS program (Microsoft) and OPUS (Bruker).

Quantum chemical calculations

Quantum chemical calculations[54] were performed with complete optimization of geometric parameters by means of minimization of energy within the frameworks of Chem Office 2004 using MOPAK software. Evaluation of charges at the atoms and interaction energy was performed with GAUSSIAN semiempirical approach in DFT approximation.[58]

Free volume measurements

Positron Annihilation Life-Time Spectroscopy (PALS)[56] was used to assess the number density and size distributions of free-volume holes in polyelectrolyte complex PSA as a function of temperature. For PALS measurements, the polymer films were prepared by dissolving the mixture of polymers in ethanol followed by casting the solution onto aluminum plates and drying for 2 days at ambient temperature (20–22°C). Films were subsequently dried for 7 days under vacuum at 28°C. PALS experiments were performed using positron sources both by a ^{22}Na-radioisotope and by a variable mono-energy 30 keV positron beam at the Kiel University (Germany).

Differential scanning calorimetry

Differential Scanning Calorimetry (DSC) was used to characterize the phase state of the polyelectrolytes and their blends. In the DSC apparatus the samples were first quench cooled with liquid nitrogen from ambient temperature to −150°C, subjected to isothermal annealing at this temperature and then heated up to 220°C at a rate of 20°C min^{-1}. The DSC heating traces were measured with a Mettler TA 4000/DSC 30 thermoanalyzer (Greifensee, Switzerland), calibrated with indium and gallium. In the DSC measurements the samples of 5–15 mg were sealed in standard aluminum pans supplied with pierced lids so that absorbed moisture could evaporate upon heating. An argon purge (50 mL min^{-1}) was used to avoid moisture condensation at the sensor. All reported values of DSC thermograms are the average of replicate experiments varying less than 1–2%.

Potentiometric titration

Potentiometric titration was performed with Ecotest-120 pH-meter, obtained from Econix (Moscow, Russia). For determination of gram equivalents of the HCl and NaOH needed for complete ionization of polyelectrolytes, the polyelectrolyte analyte was first dissolved in 1 : 1 mixture of ethanol with distilled water and obtained 1% solution was then titrated by 0.2*N* HCl or 0.1*N* NaOH aqueous solutions. Titration curves had a characteristic sigmoid shape. The section of the curve that demonstrates the maximum pH change marks the equivalence point of the titration.

Adhesive properties

Adhesive properties were studied with probe tack tests as earlier described[59] using TA.XT.plus texture analyzer from Stable Micro Systems (Godalming, Surrey, UK) equipped with thermal chamber for measurements at temperature above and below ambient. The probe tack test can be divided in two stages. The first stage is compression where the flat stainless steel probe of 4 mm in diameter penetrates into adhesive film with constant rate of 0.1 mm s^{-1} and stops, when compressive bonding stress achieves a value of 0.8 MPa. After 1 s of a contact, the probe is detached from the adhesive layer at a constant rate of 0.1 mm s^{-1}. Compliance of the probe tack tester was 9.79 μm N^{-1}.

The probe used in this test was a standard, cylindrical, polished stainless steel probe obtained from Stable Micro Systems. The probe was cleaned with acetone after each test. Such cleaning procedure was adequate to obtain meaningful and reproducible results. Force vs. time and displacement vs. time curves were thus directly obtained from this test.

For each experimental condition, we carried out three to five tests. The specific stress–strain curves shown in this article are representative of one of these individual tests while the mechanical parameters such as the maximum stress σ_{max} and the maximum extension ε_{max} are average values.

Rheological properties in the linear viscoelastic regime

Rheological properties in the linear viscoelastic regime were measured on a parallel plate Dynamical Mechanical Analyzer DMA 861 from Mettler Toledo (Greifensee, Switzerland).[59] The amplitude of shear deformation was chosen to be in the linear regime of the elastic modulus G' over the whole range of temperatures. This zone corresponded to a deformation of 3 μm. All DMA measurements were performed at the temperatures ranged from −80 to 100°C and at 1 Hz frequency. The heating rate was 3°C min^{-1}.

Tensile strain–stress behavior

Tensile strain–stress behavior of the polyelectrolyte complex adhesive films was studied with the

TA.XT.plus texture analyzer at ambient temperature. Dumbbell-shaped samples of the total length of 21 mm with a nip-to-nip distance of 10 mm were cut from the films of 0.5–0.7 mm in thickness. The width of a necked region was 5 mm. The tensile strength of the samples was determined at fixed cross head speed ranging from 10 to 100 mm min^{-1}, 10 N full scale load. The nominal tensile stress was defined as a stretching force normalized by the original cross-section area of the sample.[57] The ultimate tensile strength being the maximum force applied (to breaking) divided by the cross-sectional area of the sample. Elongation at break is calculated by dividing the distance that the crosshead of the tensile tester had traveled to sample break by the original length of the sample. All reported stress–strain curves were reproduced in replicate experiments, varying less than 10%.

Relaxation properties

Relaxation properties of the polyelectrolyte complex were studied simultaneously with the evaluation of probe tack adhesion at the conditions imitating adhesive bond formation under compressive load as earlier described.[36] To evaluate the relaxation properties of adhesive material under bonding pressure and adhesion the probe tack test is most appropriate. The probe tack experiment was performed in the way, when the probe tack test includes the relaxation of compressive stress during contact formation, while the probe position (and material deformation) remains fixed with contact time. In this case, the probe test can be divided into three successive stages.

The first stage is compression, when the flat cylindrical probe approaches the adhesive layer with a constant velocity, penetrates 0.1 mm into its depth, and then stops.

The second is the stage of relaxation, when the adhesive material under the probe relaxes during the predetermined contact time (we varied contact times from 1 to 1000 s). If a shear strain is fixed and a stress relaxation occurs, the relaxation process is described by equation:

$$G_t = G_{\text{eq}} + \sum_{i=1}^{i=n} G_i \exp(-t/\tau_i) \tag{8}$$

where G_{eq} is the equilibrium relaxation modulus, τ_i is the relaxation time and G_i is the relaxation modulus associated with τ.

The third stage is debonding, when the probe is removed with a constant debonding rate of 0.1 mm/s. Nominal stress (σ_n) and strain (ε) curves are obtained using the values of the initial film thickness (h_0) and the initial contact area (A): $\sigma = F(t)/A$ and $\varepsilon = (h(t) - h_0)/h_0$.

Water-absorbing capacity

Water-absorbing capacity of the PSAs based on polyelectrolyte complexes were evaluated in the terms of swell ratio and sol fraction using gravimetric sol–gel analysis. The swell ratio (α) was calculated according to eq. (9):

$$\alpha = \frac{m_s}{m_d}, \tag{9}$$

where m_s is the weight of the swollen sample and m_d is the weight of the sample dry gel fraction. The content of the sol fraction (S, %) was calculated with eq. (10):

$$S = \frac{(m_0 - m_d)}{m_0} \cdot 100, \tag{10}$$

where m_o is the initial sample weight and m_d is the weight of gel fraction dried after swelling.

RESULTS AND DISCUSSION

Used terminology

In further description the following terminology will be used in accordance with the definitions set out below. The term "crosslinked" herein refers to a composite material containing intramolecular and/or intermolecular crosslinks, arising through noncovalent bonding of complementary functional groups in polymer chains. Noncovalent bonding includes both hydrogen bonding and electrostatic (ionic) bonding between reactive functional groups in recurring units of polybase and polyacid macromolecules. The term complex or interpolymer complex refers to the association of macromolecules of two or more complementary polymers that forms as a result of favorable interactions between their macromolecules. The term ladder-like defines the complex or the mechanism of complexation leading to the associate of complementary macromolecules, wherein specific interaction occurs between the complementary functional groups in the repeating units of polymeric backbones. Because of entropic reasons, functional groups are linked together not separately but in a cooperative manner, thus forming relatively long sequences of tough interchain bonds. The schematic structure of such complex resembles a ladder. Therefore, in polymer science literature this type of complexes is frequently referred to as "ladder-like" polycomplexes.[43,45,46,53,60,61] In general, the interpolymer complex between the film forming polymer and

the ladder-like crosslinker is formed by hydrogen bonding, electrostatic bonding, ionic bonding, or their combination. The ladder-like complexes are crosslinked due to specific interactions between reactive groups in complementary macromolecules and thus represent "networks". In the context of present description the term "network" is used interchangeably with the term "complex", but refers more specifically to the supramolecular structure of the interpolymer complex.

In the PSAs based on polyelectrolyte complexes, the same polymer component may be used as either the film-forming polymer (FFP) or as the ladder-like noncovalent crosslinker (LLC) since both the FFP and LLC represent the same class of functional polymers, which bear reactive groups, capable to hydrogen, electrostatic or ionic bonding in the repeating units of polymer backbones. Their function and role in the composition will be determined by the amount of polymer component presented in the blend. Here the component is present in the greatest quantity functions as the film-forming polymer, i.e., the difference between FFP and LLC is an issue of their concentration. While the predominant component is typically referred to as the film-forming polymer, the minor component is referred to as the ladder-like noncovalent crosslinker. Thus, for the purposes of the PSA materials based on polyelectrolyte complexes, it is not critical what polymer—polybase or polyacid—serves as the major FFP, and what serves as the LLC. Nevertheless, it must be noted that in present research the FFP is always polybase (PDMAEMA-*co*-MMA/BMA), whereas the LLC is polyacid (PMAA-*co*-EA).

The energies of intermolecular bonds in polybase–polyacid blends with and without plasticizer

As has been shown in the first paper of this series,[54] FTIR-spectroscopy allows identification of interacting functional groups in the polyelectrolyte PDMAEMA-*co*-MMA/BMA−PMAA-*co*-EA blends. To evaluate the structure and formation energies of the variety of interpolymer complexes that involve both hydrogen and ionic bonding, quantum chemical calculations have been performed. The results of quantum chemical calculations facilitate appreciably the interpretation of FTIR-spectra. Thus, they provide an explanation for the width and indented profile of several bands in FTIR-spectra indicating that this effect results from a variety of complex structures and proximity of interaction energies between the same functional groups of complementary macromolecules. Comparison of the molecular mechanisms of polybase–polyacid interaction on the values of complexation energies gives an insight into most energetically favorable interaction mechanisms between complementary functional groups of the polymers in blends.

According to the quantum analysis of more than 300 polyelectrolyte complex structures examined in our study,[54] the energy of ionic and hydrogen bonding diminishes in the order: Multicomponent complexes involving protonated aminogroup of DMAEMA (ammonium cation) in the presence of chlorine counterion with ionized or unchanged carboxyl groups and water molecules (690–520 kJ/mol) > Ternary H-bonded acid-base complexes associated with molecule of water (520–420 kJ mol^{-1}) > Binary ionic complex of carboxylate anion and ammonium cation (404 kJ mol^{-1}) > Hydrogen-bonded complex of carboxylate and ammonium ions (257 kJ mol^{-1}) > Binary H-bonded complex of uncharged carboxyl group with ammonium cation (114 kJ mol^{-1}) > Ternary H-bonded complex of uncharged carboxyl group, aminogroup and water molecule (43 kJ mol^{-1}) > Binary H-bonded complex between nonionized carboxyl and amino groups (26 kJ mol^{-1}). In this way, the ionic complexes formed with participation of charged polyelectrolyte functional groups (ammonium cation and carboxylate anion) are in 16–4 times more energetically favorable than the strongest H-bonded complexes of uncharged complementary polybase and polyacid groups. The examples of structures and energies of most typical polyelectrolyte complexes are presented in Table I. These energies control both the phase state and cohesive strength of the PSAs based on the polyelectrolyte complexes.

The PSAs based on polyelectrolyte complex represent a new generation of water-absorbing adhesive materials. For this reason, the structures including water molecules, associated with polymer functional groups, were also taken into consideration in the course of quantum chemical analysis. As it follows from Table I, molecules of absorbed water are not competitors but rather helpers for the formation of stable, energetically favorable polyelectrolyte complexes.[54]

Proton-donating capability of functional groups in the studied polyelectrolyte blends diminishes in the order: $HN^{+}(CH_3)_2^{-}$ > $HOOC^{-}$ > HO^{-}. The proton-donating capacity can be significantly improved in the presence of Cl^{-} ions, the effect of which may be appreciably inhibited if Na^{+} cations are present in the solution. Proton-accepting capability weakens in the order: Uncharged aminogroup > Carboxylate anion > Uncharged carboxyl group > Hydroxyl group.[54]

The functional groups in our model PDMAEMA-*co*-MMA/BMA −PMAA-*co*-EA system are typical of variety of polyelectrolytes that motivates fundamental significance of obtained results for the science of polyelectrolyte complexes.

TABLE I
Comparative Strength of Ionic and Hydrogen Bonding Between Amino Groups of Polybase, Carboxyl Group of Polyacid, and Hydroxyl Group of Plasticizer

Complex type	Complex structure	Formation energy, kJ/mol
Complex of uncharged carboxyl group with two ammonium cations and chlorine counterion	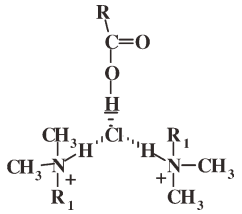	689.46
Ternary complex of uncharged carboxyl group, ammonium cation and water in the presence of chlorine counterion	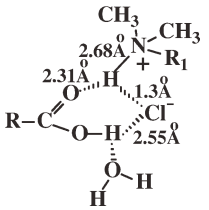	650.23
Hydrogen bonded complex of carboxylate anion and ammonium cation, stabilized with chlorine counterion	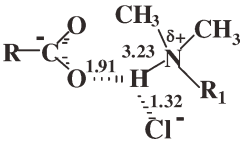	644.02
Ternary charge transfer complex of ionized carboxyl group, ammonium cation and water	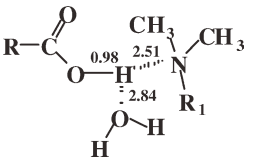	593.06
Ternary H-bonded complex of ammonium cation with carboxylate anion and water in the presence of chlorine counterion	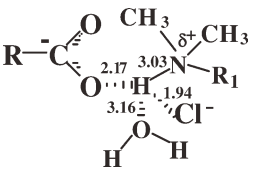	524.04
Ionic complex of carboxylate and ammonium counterions	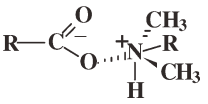	404.36
H-bonded complex of carboxylate and ammonium ions	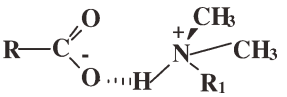	257.50
Ternary complex of uncharged carboxyl group, ammonium cation and water	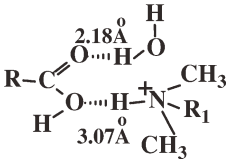	152.43
H-bonded complex of uncharged carboxyl group with ammonium cation	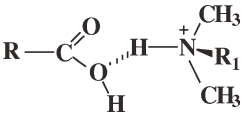	114.00

TABLE I. *Continued*

Complex type	Complex structure	Formation energy, kJ/mol
Complexes of carboxyl group and carboxylate anion	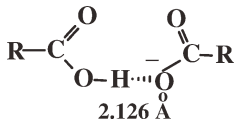	89.91
	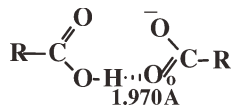	73.51
H-bonded TEC complex with carboxyl group	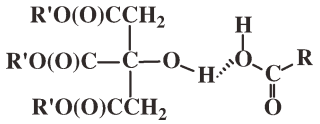	47.57
Ternary complex of uncharged carboxyl group, aminogroup and water	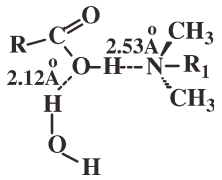	42.89
H-bonded complex between uncharged amino and carboxyl groups	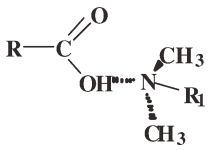	26.2
H-bonded complex of TEC with aminogroup	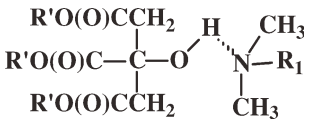	19.73

Impact of intermolecular cohesion on free nanovolume in polyelectrolyte complex PSAs

As has been noted above, strong intermolecular cohesion and cooperative mechanism of interpolymer polyelectrolyte complex formation lead to drastic decrease in the distance between neighboring complementary macromolecules and therefore to the free volume reduction. Hence, in order to reconcile the strong intermolecular bonding with large free volume, that is prerequisite of pressure sensitive adhesion,[22] special technological practice should be applied. Figure 1 presents schematic illustration of such methods.

As schematically shown in Figure 1, in blends of complementary polymers including the formation of interpolymer complexes, high cohesion energy can be provided by the formation of intermolecular hydrogen, electrostatic, or ionic bonds, crosslinking the FFP chains into three-dimensional network structures.[55] Cohesive strength of the network is controlled by the number and strength of interchain junctions. Two kinds of junctions may be distinguished. Junctions **A** represent the ladder-like sequences of interchain bonds, and their strength depends on the energy and amount of these bonds, i.e., on the length of the ladder-like bond sequences. Junctions **B** emerge owing to physical entanglements of long FFP macromolecules in the blend. Their amount and strength are affected by the FFP concentration in blend and the length of the FFP chains. Free volume in interpolymer complexes, along with other defects of the supramolecular network structure, can be produced by loops (**C**) of unbonded macromolecular chains (Fig. 1). The size and amount of loops, or the conversion degree in cooperative chemical reaction of interpolymer complex formation in solid phase, are governed by the content and the strength of polymer chain entanglements **B**. Thus, we can more likely expect that the free volume in polyelectrolyte blends will be rather provided by the

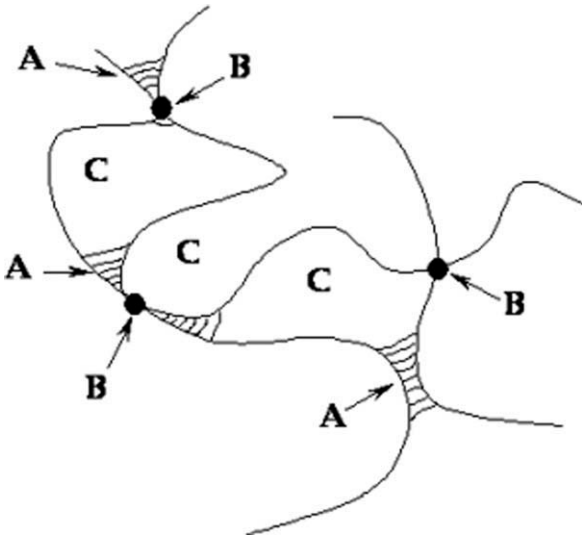

Figure 1 Schematic presentation of non-covalently crosslinked network structure of interpolymer complexes. A: Noncovalent crosslinks consisting of sequences of hydrogen, electrostatic or ionic bonds formed between functional groups in monomer units of complementary macromolecules. B: The entanglement junctions of long polymer chains and C are the loops consisting of the segments of macromolecules free of interpolymer bonding.[55]

specific features of polyelectrolyte PSA preparation method, than as a result of interpolymer bonds cohesion energy.

Really, as our most recent data of PALS measurements have shown,[56] the value of hole free volume for the polyelectrolyte complex PSA at 20°C has been found to be 179 Å^3 (±2 Å^3), whereas for others typical PSAs it ranges from 145 to 183 Å^3 (±2 Å^3). Thus, in spite of the fact that the intermolecular cohesion energy of the polyelectrolyte complex PSA is essentially higher, than for other typical representatives of the PSA family, the behavior of free volume quite conform to the values which are observed for typical PSAs of other chemical compositions.

Phase state of polyelectrolyte complex PSAs as function of intermolecular cohesion and free nanovolume

As has been shown in the second article of this series,[55] the value of glass transition temperature (T_g) is an important indicator of the ratio between the energy of intermolecular cohesion and the free volume of polyelectrolyte blends. The growth of cohesion results generally in the increase of T_g value, while the rise of free volume leads to the T_g reduction. The blends of PDMAEMA-*co*-MMA/BMA polybase with PMAA-*co*-EA polyacid and TEC plasticizer exhibit occurrence of a single glass transition temperature, notwithstanding that only 20 : 1 and 10 : 1 plasticized polybase–polyacid blends are single-phase, whereas the blends of the polybase with higher amounts of the polyacid LLC display the signs of microphase separation. The composition behavior of the T_g in PDMAEMA-*co*-MMA/BMA blends with PMAA-*co*-EA and TEC demonstrates predominant contribution of a large free volume formation into T_g value. It is surmised that polyelectrolyte mixing in a solid state or in concentrated solutions, which leads to polymer chain entanglements, favors the formation of the loops of polymer chains, which are free of intermolecular bonding.

Ionization of polyelectrolyte functional groups affects appreciably the phase state of unblended components but has only inappreciable impact on the T_g behavior in the blends. Measured T_g values are in fairly reasonable correlation with earlier established mechanisms of molecular interaction in the PDMAEMA-*co*-MMA/BMA blends with PMAA-*co*-EA and TEC as a plasticizer.[54,55]

Mixing the polybase with the polyacid in solution, in vicinity of 1 : 1 concentration ratio, results in formation of a sol and gel fractions. The sol fraction consists predominantly of the nonstoichiometric complex of so-called "scrambled egg" structure. In contrast, the gel fraction represents the stoichiometric ladder-like network polyelectrolyte complex. The T_g values are always higher for the stoichiometric ladder-like complex than for the nonstoichiometric polyelectrolyte complexes of the "scrambled egg" structure. This fact is a direct confirmation that intermolecular cohesion dominates free volume in the stoichiometric ladder-like polyelectrolyte complex, while in the slightly crosslinked nonstoichiometric complexes of "scrambled egg" structure, the free volume dominates the energy of intermolecular cohesion due to loop formation. When the stoichiometric and nonstoichiometric polyelectrolyte complexes are not separated by the filtration of casting solution prior to dry blend preparation, the "scrambled egg" complex forms continuous phase of lower T_g, while the finely divided particles of the ladder-like complex in dispersed phase with upper T_g have microscopic sizes and do not show separate T_g value. Supramolecular structures of nonstoichiometric and stoichiometric polyelectrolyte complexes have been studied with electron microscopy. Nonstoichiometric "scrambled egg" complex in sol phase exhibits lamellar structure, while stoichiometric ladder-like complex in gel phase forms well-developed fibrillar network structure that resembles a nanosized web.[55]

State diagram of polybase–polyacid blends reveals the areas of partial component miscibility and the formation of the nonstoichiometric complex of "scrambled egg" structure, which are separated by a field occupied by the ladder-like polyelectrolyte complex of stoichiometric composition that is immiscible with both parent polymers at temperatures

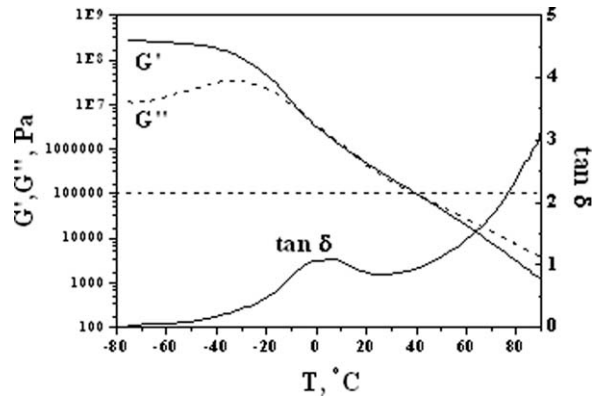

Figure 2 Temperature behaviors of the storage modulus G', loss modulus G'' and tan δ for the PSA based on plasticized polyelectrolyte complex. The PSA represents 20 : 1 polybase–polyacid blend with 45 wt % TEC plasticizer. Reference deformation frequency is 1 Hz.

below 172°C. Melting of the ladder-like complex and polybase–polyacid miscibility above this critical temperature is thought to be result from the complex dissociation at high temperatures, when intermolecular hydrogen bonds do not exist any longer. The plasticized polybase–polyacid blends of 20 : 1 and 10 : 1 concentration ratios, demonstrating pressure sensitive adhesion, relate to the area of the phase diagram which corresponds to the nonstoichiometric polyelectrolyte complex of the "scrambled egg" structure. The stoichiometric ladder-like polyelectrolyte complex in the blends of 1 : 1 polybase–polyacid composition ratio with plasticizer exhibits no adhesion.

Linear viscoelastic properties of the polyelectrolyte PSAs

Let us consider now macroscopic physical properties of the polyelectrolyte PSAs. As DMA data demonstrate in Figure 2, glass transition of the polyelectrolyte complex based PSA occurs at −35°C. At this temperature the loss modulus curve (G'') reveals a maximum and the curve of storage modulus (G') shows an inflection point. Loss tangent peak (tan δ = 1.13) is observed at 6°C. Distinctive feature of PEC-based PSA is a lack of viscoelasticity plateau. This behavior is explicable, because with an increase in temperature the interpolymer bonds, forming three-dimensional noncovalent network, become looser and finally break. Accordingly, the blend transforms into fluid state.

As seen from Figure 2, the storage modulus achieves the values below 0.1 MPa at temperatures above 40°C. According to well-known the Dahlquist criterion of tack, within this particular temperature range we can expect the best adhesive properties of the polyelectrolyte blends. The Dahlquist criterion stipulates that the shear elastic modulus G' at bonding frequency of 1 Hz must be lower than 0.1 MPa for an adhesive layer to be able to form a good adhesive contact with a substrate within the contact time of 1–5 s and, consequently, to exhibit good adhesive strength.[62] At ambient temperatures, the contribution of the energy of intermolecular cohesion in the polyelectrolyte complex dominates that of the free volume. Elevation of temperatures leads to loosing of noncovalent bonds, shifting the balance between cohesion strength and free volume towards domination of the latter, and creates conditions favoring the pressure sensitive adhesion. Temperature relationship of probe tack adhesion in the polyelectrolyte complexes is considered in section "Temperature Relationship of Adhesion" of this article.

Large-strain tensile properties of the polyelectrolyte PSAs

The PSAs based on polyelectrolyte complexes contain three obligatory components: the film-forming polymer (FFP, which is the polybase PDMAEMA-*co*-MMA/BMA in our particular case), its noncovalent ladder-like crosslinker (LLC, PMAA-*co*-EA polyacid) and plasticizer (TEC). As it is noted above, direct correlation occurs between adhesion and large-strain tensile properties of the PSAs. In this way, consideration of the tensile behavior of the PSA allows us to establish and illustrate the role and function of each component in the polyelectrolyte blend. Since stretching is the main type of deformation of PSAs during adhesive joint failure,[25–28,63] the study of the mechanical characteristics of polymer materials during the uniaxial drawing to break is of utmost importance.

As is seen from Figure 3, the stress–strain curve for the binary blend of the FFP (polybase) with 25

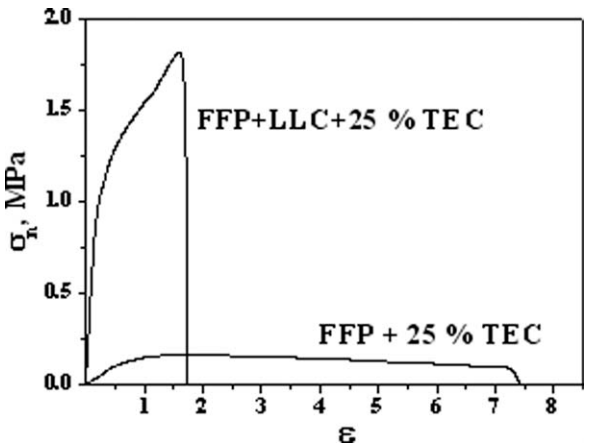

Figure 3 Nominal stress–strain curves for uniaxial drawing of the mixture of FFP with 25 wt % TEC plasticizer and the nonstoichiometric polyelectrolyte complex ([FFP]:[LLC] = 10 : 1) plasticized with the same amount of TEC. Drawing rate is 20 mm/min.

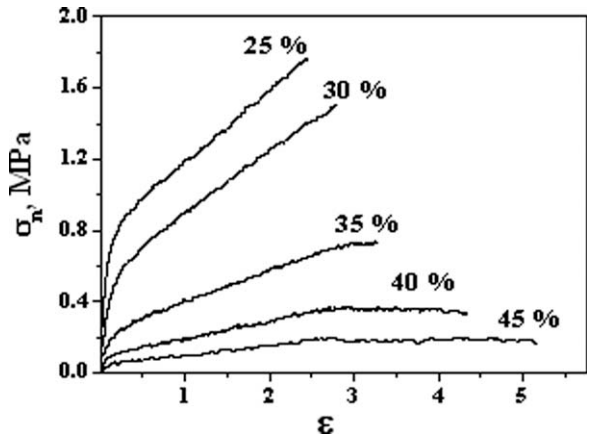

Figure 4 Effect of plasticizer concentration on tensile stress–strain curves of polyelectrolyte blends (FFP/LLC = 10/1). TEC content is indicated. Drawing rate is 20 mm/min.

wt % plasticizer is typical for the deformation of viscoelastic liquids, such as entangled linear macromolecules and noncrosslinked rubbers. The incorporation of even small amounts of the polyacid (PMAA-*co*-EA; polybase : polyacid = 10 : 1) causes dramatic changes in the type of deformation and in the profile of the curve. This type of extension becomes typical for densely crosslinked rubbers. In this case, the breaking strength of the films grows by a factor of 6.6, while the maximum elongation decreases by a factor of 4.3. The ultimate stress at fracture is a direct measure of the cohesive strength of the deformed material, whereas the maximum elongation at break is proportional to the content of free volume, as measured by positron annihilation spectroscopy.[42]

Our experimental data show that the polyacid in the blend with polybase plays the role of the noncovalent ladder-like polymer crosslinker (LLC), thereby increasing the cohesive strength of the material and decreasing its free volume.

Figure 4 illustrates the effect of the plasticizer content on the tensile stress–strain curves of the polyelectrolyte blend. The stress–strain curves for the blend under study are similar in shape to the corresponding curves for lightly crosslinked elastomers, among which are all PSAs. This is manifested by high ultimate strains (ε_b) typical for rubbers, as well as the occurrence of ductile or "plastic flow" regions characteristic of plastic deformation. As has been earlier shown under phase state study of the polyelectrolyte complexes,[55] TEC is a good plasticizer of PDMAEMA-*co*-MMA/BMA blends with PMAA-*co*-EA. This conclusion is now confirmed by the analysis of tensile stress–strain curves. With an increase in the concentration of plasticizer, the ultimate tensile strength and the work of viscoelastic deformation to break (the area under the stress–strain curve) decrease, whereas the maximum elongation increases. Pertinently to remind once again, that both former values are the indirect measures of cohesion strength, whereas the latter relates directly to the content of free volume.[42]

In this manner, varying the composition of FFP–LLC blends with plasticizer provides easy tuning of mechanical properties. The ultimate strength and ductility of the blends are such that they can be useful in many practical applications.

Alternative tool to manipulate tensile properties of the nonstoichiometric polyelectrolyte complex PSA is varying the drawing rate. As follows from comparison of the tensile stress–strain curves (Figs. 4 and 5), the effect of increase in plasticizer concentration is equivalent to the effect of decrease in stretching rate. The effect of deformation rate is a manifestation of the contribution of relaxation to large strain mechanical properties and adhesion of the polyelectrolyte PSA, which is considered in following sections of this research article. The relationship between adhesion and relaxation properties of the PSAs follows from eq. (6) presented in Introduction.

Adhesion of the PSAs based on nonstoichiometric polyelectrolyte complexes

Impact of PSA free volume and cohesion strength on Probe Tack curves

In development of novel PSAs, Probe Tack Test is a most informative and highly illustrative tool that enables not only characterizing an adhesive joint strength, but also gaining a qualitative insight into relative contributions of the cohesive molecular interaction energy (E_c) and the free volume (f_v) to adhesion. As E_c contribution dominates that of f_v, Probe Tack curve has a shape illustrated in Figure 6 by the Curve 1, which is typical for debonding of

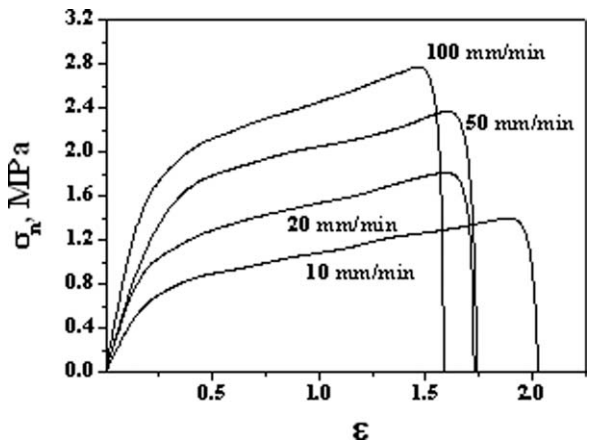

Figure 5 Effect of drawing rate on tensile stress–strain curves of 10 : 1 PDMAEMA-*co*-MMA/BMA–PMAA-*co*-EA complex containing 45 wt % TEC plasticizer.

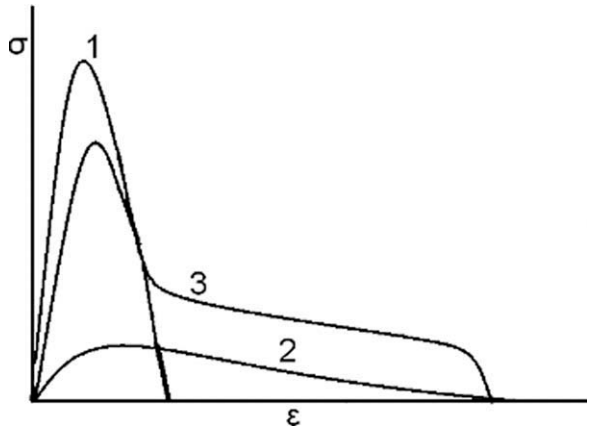

Figure 6 Typical Probe Tack curves for solid-like PSA (high E_c/f_v ratio; Curve 1), liquid-like adhesive (low E_c/f_v ratio; Curve 2) and the PSA with optimized adhesion (intermediate value of E_c/f_v ratio, Curve 3).

solid-like PSAs. This curve is characterized by a sharp maximum at rather low strains and a very small area under the stress–strain curve. Adhesive joint failure in this case proceeds through interfacial crack propagation between the probe and adhesive film surface and is called "adhesive debonding."[59]

At the other extreme, as the f_v prevails, Probe Tack curve has a view shown by the Curve 2 (Fig. 6). This type of adhesive joint failure is characteristic feature of fluid PSAs,[64,65] which demonstrate comparatively low cohesion strength, indicated by lower peak of debonding stress (σ), coupled with relatively high value of elongation (ε). In this case, the adhesive joint breaks by the cohesive fracture within the bulk of adhesive layer, and the debonding process is governed by viscous flow. This type of debonding is also called "cohesive debonding," where some residues of adhesive are left on the probe at the end of the test.

In between these two cases, when high E_c is properly equilibrated with large f_v, the area under Probe Tack curve, defined as the practical work of adhesion, achieves its maximum value. Debonding proceeds via cavitation and fibrillation of adhesive layer, which are typical for the PSAs with optimized adhesion (Curve 3 in Fig. 6). The curve shows a peak of debonding stress followed by a more or less pronounced plateau. The curve finally ends up by a gradual or sharp decrease of detaching force to zero. Detachment in that case occurs at the interface between the probe and the adhesive layer.[65] No macroscopic residue occurs on the probe at the end of the test. When material strain-hardening in fibrils is observed just before the final detachment, the Probe Tack stress–strain curve can demonstrate a slight increase in the stress or a second peak.

Effect of noncovalent polymer crosslinker

The probe tack profiles (Fig. 7) are informative on the mechanism of debonding process. The PSAs are known to couple the properties of liquid-like and solid-like materials and the shape of the stress–strain curves illustrates qualitatively this dualism. In probe tack curves, the liquid-like behavior relates to the material capability of developing very high values of maximum elongation ($\varepsilon \approx 10$–40) under comparatively low levels of applied detaching stress (less then 0.1 MPa). In contrast, solid-like behavior is evident when debonding occurs at relatively small values of maximum elongation ($\varepsilon < 1$) and is provided by high values of debonding stress.

Figure 7 illustrates the effect of LLC on probe tack curves of the polyelectrolyte complex at two concentrations of plasticizer 25 and 35 wt % TEC. As follows from the curves (Fig. 7), the ladder-like noncovalent cross-linking of FFP (PDMAEMA-*co*-MMA/BMA polybase) with LLC (PMAA-*co*-EA polyacid) results in a dramatic change in debonding mechanism, from that typical of liquid PSAs (observed for

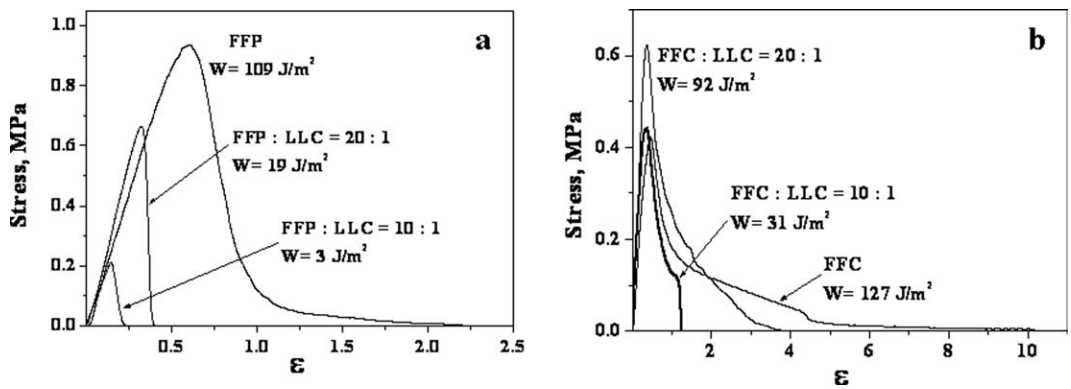

Figure 7 Probe tack curves of the PDMAEMA-*co*-MMA/BMA polybase (FFP), and its polyelectrolyte complexes with LLC (polyacid, PMAA-*co*-EA). FFP:LLC = 20 : 1 and 10 : 1. The rate of probe detachment is 0.1 mm/s. Corresponding values of the practical work of adhesion (debonding energy) are indicated in the Figure. A: 25 wt % of TEC plasticizer. B: 35 wt % of TEC plasticizer.

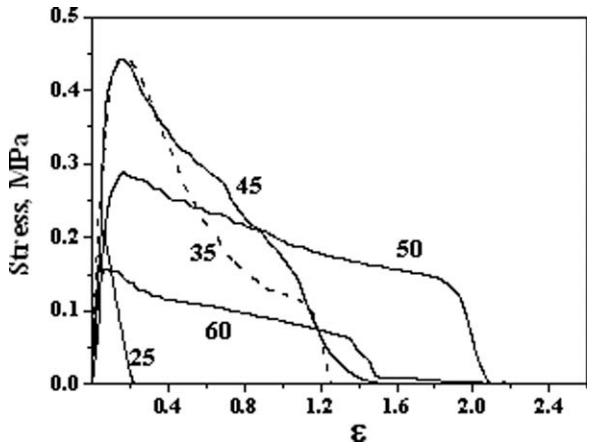

Figure 8 Effect of triethyl citrate concentration on the deformation mechanism of the adhesive layer in the 10 : 1 polyelectrolyte complex of PDMAEMA-*co*-MMA/BMA with PMAA-*co*-EA. The rate of probe detachment is 0.1 mm/s. The TEC concentrations are indicated in Figure.

plasticized FFP) to more elastic and solid-like, featured for ternary PDMAEMA-*co*-MMA/BMA blends with PMAA-*co*-EA and TEC. Such LLC behavior, observed also on the data of tensile test (compare Figs. 7 and 3), implies the domination of intermolecular cohesion over the free volume (Fig. 6).

In Probe Tack curves, the stress peak relates to the cavitation of the adhesive material under detaching tensile force.[26,27,66] The major factor providing dissipation of a great amount of energy in the course of debonding of PSAs is the fibrillation of the adhesive layer, which is observed by the appearance of a plateau on stress–strain curves. Adhesive joints of solid adhesives fail predominantly via the mechanism of cavitation that is not followed by fibrillation. The typical shape of their probe tack stress–strain curves is a symmetric peak. In the probe tack experiment, the maximum stress is generally considered as a measure of tack, the value of plateau stress characterizes the cohesive strength of fibrils, and the area under the stress–strain curve relates to the total amount of mechanical energy needed for adhesive bond failure. In this way, the value of practical work of adhesion (W) is a measure of adhesive strength.

As illustrated in the Probe Tack curves [Fig. 7(a,b)], a binary blend of PDMAEMA-*co*-MMA/BMA containing 25 and 35 w/w% of plasticizer TEC and no polyacid cross-linker is a tacky liquid that debonds cohesively at relatively high values of elongation, leaving significant amount of adhesive at the surface of the probe. The higher the TEC concentration, the more the PSA is liquid-like that is obvious from the values of maximum adhesive layer stretching in the point of debonding, ε_{max}. At 35 wt % TEC in blend, mixing the FFP with complementary LLC in the ratios of [FFP]:[LLC] = 20 : 1 and 10 : 1 leads to an immediate change in the debonding mechanism from cohesive to adhesive. Ladder-like crosslinking of FFP decreases the work of debonding from 126 to 92 and 31 J m^{-2}, respectively. The 20 : 1 nonstoichiometric polyelectrolyte complex demonstrates the better balance between elastic and plastic behaviors. Although debonding energy is somewhat decreased as compared with uncrosslinked FFP, this lightly crosslinked PSA exhibits adhesive type of debonding. Further increase of the LLC concentration results in following decrease of both maximum debonding stress and adhesive layer stretching. Thus, domination of the cohesion interaction over free volume space is produced by the ladder-like cross-linking of FFP, which affects the adhesion properties.

Effects of plasticizers and tackifier

As is seen from Figure 8, upon introduction of plasticizer into the PDMAEMA-*co*-MMA/BMA–PMAA-*co*-EA polyelectrolyte complex, the deformation mechanism typical of solid adhesives (25 wt % TEC) changes to that inherent to viscoelastic adhesives. With an increase in the plasticizer concentration, the maximum stress of debonding grows, passes through a maximum at 35–45 wt % TEC, and finally declines (Fig. 9). The appearance of the plateau in the Probe Tack curves indicates the contribution of adhesive layer fibrillation. The maximum elongation of fibrils tends to increase with an increase in the plasticizer content (Fig. 9). As it has been recently shown in[42] for a PSA based on polymer–oligomer complex of high-molecular weight poly(*N*-vinyl pyrrolidone) with short-chain poly(ethylene glycol), the value of maximum stretching of adhesive layer in the course of debonding process increases linearly with the increase of free volume content. The work of adhesive joint failure passes through a maximum at 50–55 wt % of plasticizer (Fig. 10). At the same

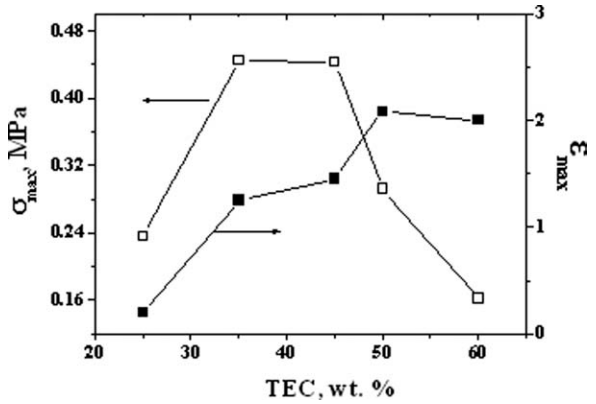

Figure 9 Impact of plasticizer concentration on the values of maximum debonding stress (σ_{max}) and maximum adhesive layer stretching (ε_{max}) for the PSAs based on 10 : 1 polyelectrolyte complex.

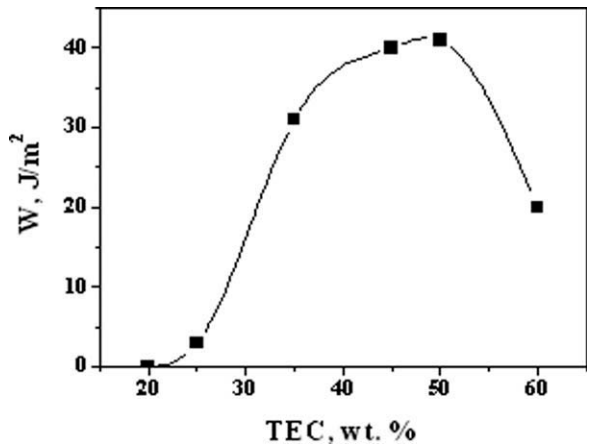

Figure 10 The practical work of adhesion as a function of TEC concentration in FFP:LLC = 10 : 1 polyelectrolyte complex.

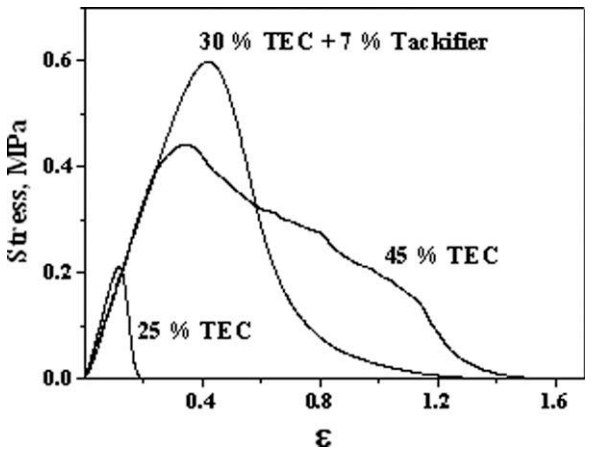

Figure 12 Comparative effects of plasticizer (TEC) and tackifier on Probe Tack stress–strain curves of adhesives based on the polyelectrolyte complex (FFP : LLC=10 : 1).

time, the Probe Tack curve obtained for the blend containing 50 wt % of plasticizer suggests the adhesive type of adhesive joint failure and indicates that, for the blend containing 60 wt % TEC, detachment of the adhesive layer from the steel probe surface proceeds according to the cohesion mechanism. The adhesive bond failure in the Probe Tack curves manifests as a sharp drop of the debonding stress, whereas the cohesion mechanism is characterized by a gradual decrease in the stress of probe debonding in the final section of the curve (Fig. 8).

As it is clear from Figure 11, the hydrophilicity of the plasticizer significantly affects the failure mechanism of adhesive joints of the FFP–LLC polyelectrolyte complex. The higher is the plasticizer hydrophilicity, the higher the adhesion. The work of probe detachment from the adhesive film surface grows with an increase in plasticizer hydrophilicity in the sequence: acetyltributyl citrate (ATBC) < tributyl citrate (TBC) = acetyltriethyl citrate (ATEC) ≈ triethyl citrate (TEC). If blends with hydrophobic plasticizers (ATBC and TBC) behave as solid adhesives and are destroyed without fibrillation of the adhesive layer, the blends of the polyelectrolyte complex with hydrophilic plasticizers (ATEC and TEC) demonstrate the existence of fibrillation, which is most pronounced in the case of the most hydrophilic plasticizer—TEC.

Owing to the presence of an appreciable amount of hydrophobic monomer units in cationic PDMAEMA-*co*-MMA/BMA and anionic PMAA-*co*-EA copolymers, adhesives based on acid–base polymer complexes are miscible with nonpolar tackifiers (rosins) and conventional acrylic PSAs employed in the adhesive industry. As illustrated by the Probe Tack curves (Fig. 12), the addition of tackifier (glycerol ester of tall oil rosin) improves significantly the tack of plasticized ladder-like polyelectrolyte complex.

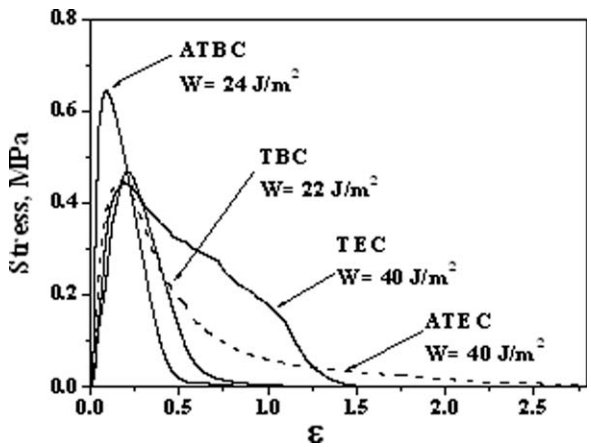

Figure 11 Impact of plasticizer hydrophilicity upon Probe Tack curves of the blends composed of the 10 : 1 polybase complex with polyacid. Plasticizer content is 45 wt %.

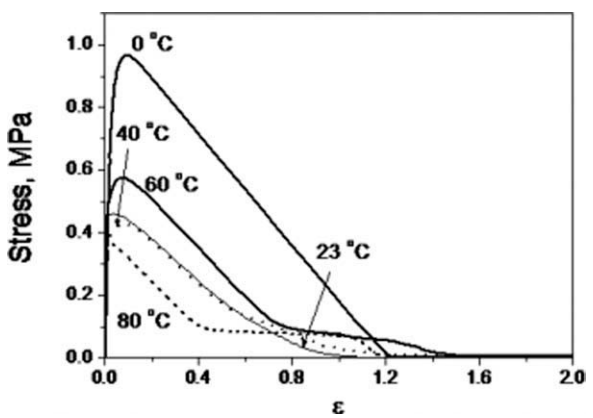

Figure 13 Effect of temperature on Probe Tack curves of the PSA based on 20 : 1 polybase–polyacid blend with 45 wt % TEC plasticizer. Debonding rate is 0.1 mm/s.

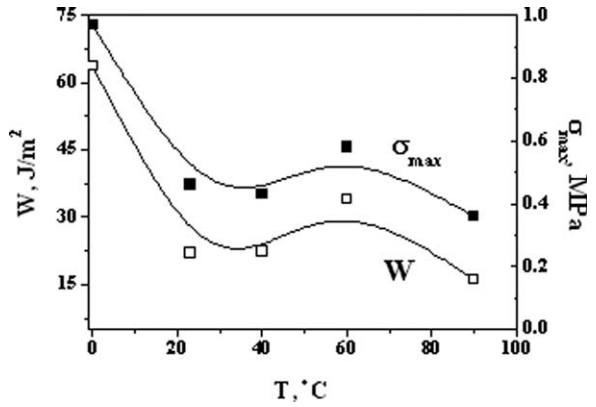

Figure 14 Maximum debonding stress (σ_{max}) and practical work of adhesion (W) as functions of temperature for 20 : 1 polyelectrolyte complex with 45 wt % TEC plasticizer.

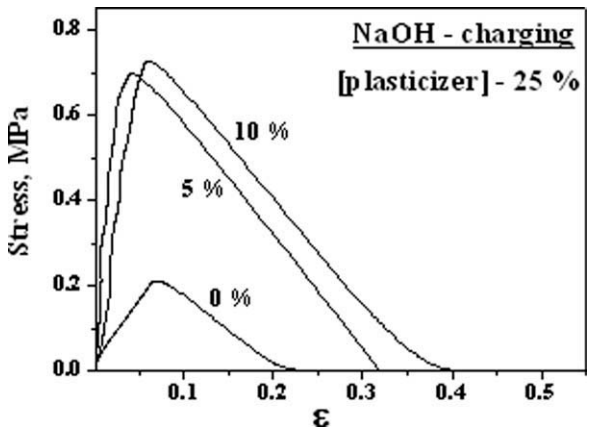

Figure 16 The effect of partial ionization of LLC by NaOH solution on the tack of polyelectrolyte complex containing 25 wt % plasticizer TEC.

Temperature relationship of adhesion

As is noted in section "Linear Viscoelastic Properties of the Polyelectrolyte PSAs" of this article, based on comparison of temperature dependence of the storage modulus of the polyelectrolyte complex with the values predicted with the Dahlquist criterion of tack, the best adhesive properties of the polyelectrolyte blends can be expected at temperatures above 40°C. Let us check this supposition.

Figure 13 illustrates Probe Tack curves of the polyelectrolyte PSA at different temperatures of debonding. At 0°C brittle-like mechanism of adhesive joint failure is observed. Elevation of temperature till 23°C leads to brittle–ductile transition and the onset of fibrillation process, which is evidenced by appearance of a plateau in Probe Tack curves. At temperatures relating to elastic type of the polyelectrolyte PSA deformation in the course of debonding, the maximum strength of adhesive joint is observed at 60°C (Fig. 14). We do not consider and discuss here the reasons behind high values of practical work of adhesion at low temperatures, because it was done in Ref. [59]. Really, the PSAs are viscoelastic polymers, functioning at 40–100°C above their glass transition temperatures. The behavior of PEC-based PSA satisfies this requirement only above 30°C. Temperature relationship of debonding stress peak (σ_{max}) follows the pattern shown by the practical work of adhesion (W, Fig. 14).

When the viscoelastic behavior in Figure 2 is compared with that of adhesion (Figs. 13 and 14), it is apparent that the brittle–ductile transition at 23°C relates to $G' = 0.34$ MPa and tan $\delta = 0.85$. Correspondingly, maximum of adhesion has been established to occur at $G' = 0.02$ MPa and tan $\delta = 1.41$, i.e., in an area predicted with the Dahlquist criterion of tack. Thus, although chemical composition of the polyelectrolyte complex PSA has nothing to do with the composition of typical PSAs, the adhesion behavior of this innovative PSA is described by the same general lows, which are established for classical PSAs.[59]

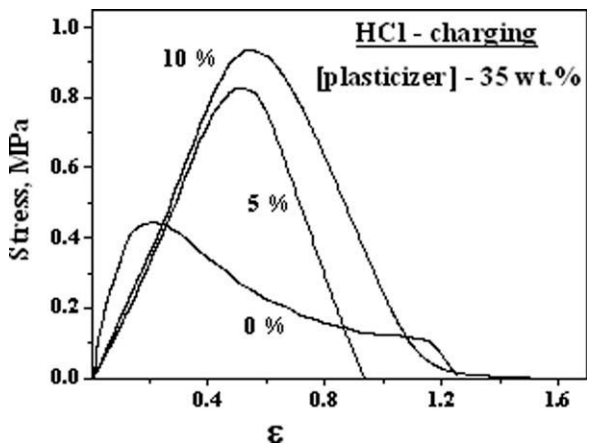

Figure 15 The effect of partial ionization of amino groups in PDMAEMA-*co*-MMA/BMA copolymer on Probe Tack curves of a ladder-like interpolymer complex plasticized with TEC. Ionization degrees are indicated in Figure.

Impact of the type of intermolecular bonds on adhesion of polyelectrolyte complexes

Partial ionization of polybase or polyacid in the blend, achieved with the addition of a strong inorganic acid (HCl) or base (NaOH), also improves the adhesive properties and changes the mechanism of debonding from fibrillar to solid-like (Figs. 15–17). The implication of these Probe Tack data is that the adhesive properties are affected by a mechanism of specific interaction between the components of the polyelectrolyte complex (hydrogen or ionic bonding), which governs the structure of the complex and determines the balance between cohesion energy and free volume. The electron-donating

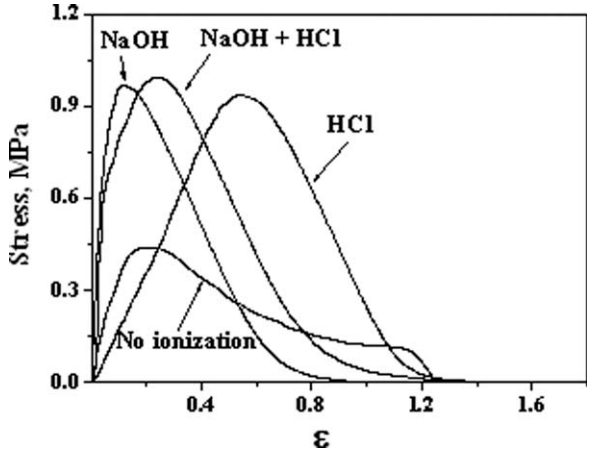

Figure 17 Effect of way of ionization of components of polyelectrolyte complex on Probe Tack stress–strain curves. TEC content was 35 wt %.

amino groups of PDMAEMA-*co*-MMA/BMA polybase are capable of forming hydrogen bonds with the proton-donating carboxylic groups of PMAA-*co*-EA polyacid (see section The Energies of Intermolecular Bonds in Polybase–Polyacid Blends with and Without Plasticizer, Table I)[54]:

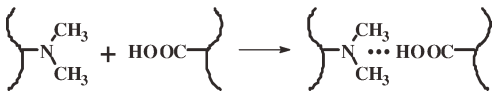

According to the quantum chemical modeling data listed in Table I, such H-bonded complexes of uncharged complementary functional groups are characterized with formation energy of $\sim$ 26 kJ/mol. Inclusion of water molecule into the bonding makes the complex more stable (ΔE = 43 kJ mol^{-1}). Treatment of PDMAEMA-*co*-MMA/BMA by HCl in aqueous solution causes partial ionization of the polybase and the formation of ammonium cations, which can interact with the carboxyl groups of PMAA-*co*-EA through the exchange reaction[37,54]:

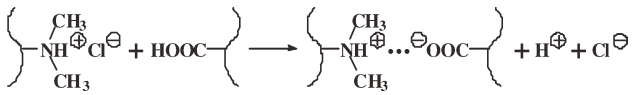

Ionic bonds are much stronger than the hydrogen bonds (Table I). Their energy ranges between 251 and 404 kJ mol^{-1}, and involving of the associated water molecule into the ionic complexes enhances intermolecular bonding energy up to 524–650 kJ mol^{-1}.[54] As the data presented in Figure 15 illustrate, the increase in the energy of interpolymer bonding leads to the increase in both the energy of cohesion and adhesion. This allows us to suppose that the free volume in the LLC involving ionic bonds increases accordingly. Electrostatic repulsion of cationic ammonium groups in ionized PDMAEMA-*co*-MMA/BMA macromolecule leads to the increase in free volume.

Partial neutralization of the carboxylic groups of LLC (PMAA-*co*-EA–polyacid) by treatment with NaOH solution, results in the formation of carboxylate anions that are unable to interact with uncharged amino groups of FFP (PDMAEMA-*co*-MMA/BMA–polybase) and therefore do not contribute to the increase in cohesion energy. However, electrostatic repulsion between these anions increases the free volume. As a result, adhesion increases, illustrated by Probe Tack data (Fig. 16). Finally, the combined effect of ammonium cations in FFP and carboxylate anions in the LLC enhances adhesion (Fig. 17).

The PSAs based on ionic polyelectrolyte complexes, described in this section, represent an example of "smart" pH-responsive PSAs. They can be employed in various areas of industry and in medicine as electroconductive adhesives.

Impact of the nature of noncovalent polymer crosslinker

PDMAEMA-*co*-MMA/BMA polybase and PMAA-*co*-EA polyacid are not unique FFP and LLC suitable for the preparation of adhesives based on the mechanism of the ladder-like polyelectrolyte complex formation. As Figure 18 illustrates, replacement of PMAA-*co*-EA polyacid by the copolymer of maleic acid with methylvinyl ether (PMA-*co*-MVE) increases adhesion appreciably, implying that the approach illustrated in this research article has a general character.

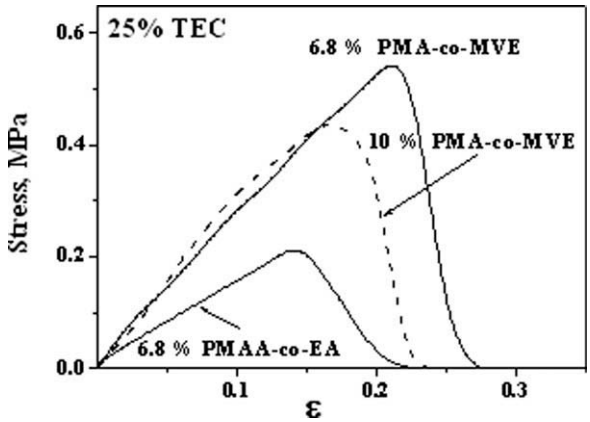

Figure 18 Probe Tack behavior of interpolymer complexes containing the ladder-like cross-linkers of different hydrophilicity and hydrogen-bonding capability: PMAA-*co*-EA and PMA-*co*-MVE. TEC content in blends was 25 wt %.

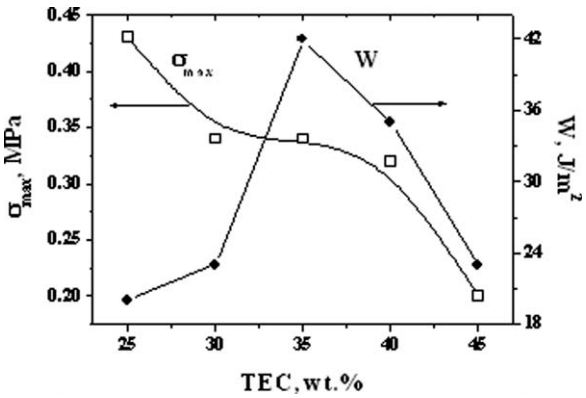

Figure 19 Values of maximum debonding stress and the practical work of adhesion vs. plasticizer concentration for PSA adhesive based on a polybase–polyacid complex. Contact time is 1 s, debonding rate is 0.1 mm s^{-1}.

Relaxation and adhesion of polyelectrolyte complexes

Effect of plasticizer concentration

Figure 19 illustrates the influence of TEC content on the values of maximum stress and the practical work of adhesion for the interpolymer complex. Whereas σ_{max} is a decreasing function of the plasticizer content, the work of adhesion passes through a maximum at 35 wt % TEC. The adhesive behavior of the blend with 35 wt % TEC corroborates the fact that the pressure-sensitive type of adhesive behavior requires a specific balance between solid-like and liquid-like properties.

Relaxation curves obtained in the course of adhesive joint formation between an adhesive layer and a probe are illustrated in Figure 20. The results of fitting the relaxation curves with eq. (8) are presented in Table II. There is a sharp transition in the relaxation behavior of the blends that contain 30 and 35 wt % of TEC. Although the interpolymer complexes containing 25 and 30 wt % TEC demonstrate a highly pronounced residual stress on the relaxation curves, which is a characteristic feature of cross-linked and ordered structures, the relaxation curves of the polyelectrolyte blends with 35 wt % TEC and more demonstrate a gradual decrease in stress that is rather typical of viscous liquids. Adequate fitting of the relaxation curves in Figure 20 with eq. (8) is possible using a sum of three exponents. The effect of TEC concentration on relaxation times is illustrated in Figure 21. The longer relaxation time is a decreasing function of plasticizer content. Accordingly, the values of the equilibrium relaxation modulus reduce with the increase in TEC concentration (Table II). Faster relaxation processes, τ_1 and τ_2, are unaffected by the concentration of the plasticizer (Fig. 21) that controls the adhesive properties (compare with the data in Fig. 19). On the basis of this observation, a logical deduction can be drawn that the large-scale relaxation processes, characterized by the value of the longer relaxation time, contribute more to the polyelectrolyte PSA performance. This experimental conclusion confirms theoretical prediction made on the basis of eq. (6), signifying the importance of the longer relaxation times for high pressure-sensitive adhesion.

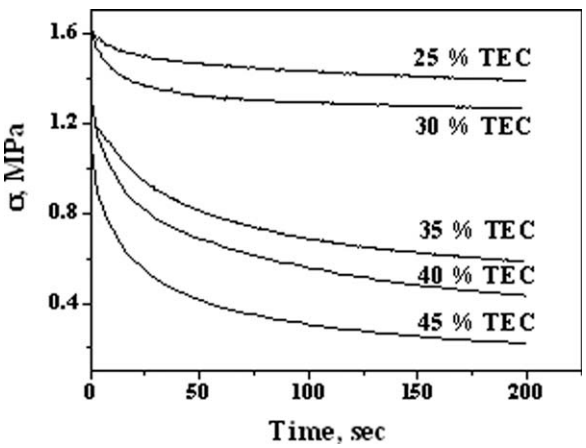

Figure 20 Relaxation curves obtained in the course of adhesive joint formation for the polyelectrolyte complex with different amounts of plasticizer (TEC). Contact time is 200 s.

Effect of contact time on adhesion

Figure 22 illustrates the impact of contact time on the typical curve of nominal compressive stress relaxation during adhesive bond formation, followed by the debonding process, for the model adhesive based on polyelectrolyte complex and plasticized with 35 wt % TEC. The variation in contact time does not change the mechanism of the debonding process. The curve presented in Figure 22 is typical and relates to the blend that exhibits the best adhesion (compare with Fig. 19).

Figures 23 and 24 demonstrate the effect of contact time on the value of the practical work of adhesion and maximum stress. Both σ_{max} and W achieve their limiting values at contact times about $\sim$ 50 s. This time corresponds to the beginning of the domination of slow relaxation processes (compare with Fig. 20) and, as a consequence, to the onset of large-scale rearrangements within the supramolecular structure of the adhesive network polyelectrolyte complex. However, this tendency is less pronounced for the blend that contains 45 wt % TEC (Figs. 23 and 24). Indeed, this blend exhibits a liquid-like behavior that is characterized by a faster relaxation. The σ_{max} values increase with increasing contact time, whereas the increase in plasticizer concentration in the polyelectrolyte complex results in a decrease of maximum stress values (Fig. 23). The values of σ_{max}

TABLE II
Relaxation Properties of a Model PSA Made Up of Polybase-Polyacid Nonstoichiometric Interpolymer Complex Containing Different Amounts of Plasticizer (TEC)

TEC wt %	G_{eq}, MPa	G_1, MPa	τ_1, s	G_2, MPa	τ_2, s	G_3, MPa	τ_3, s
25	1.342 ± 0.004	0.051 ± 0.003	1.29 ± 0.13	0.091 ± 0.002	12.54 ± 0.56	0.164 ± 0.002	161.12 ± 8.35
30	1.238 ± 0.004	0.110 ± 0.004	2.84 ± 0.13	0.186 ± 0.003	16.29 ± 0.57	0.106 ± 0.002	145.8 ± 15.18
35	0.515 ± 0.003	0.135 ± 0.002	0.66 ± 0.02	0.314 ± 0.006	20.83 ± 0.38	0.415 ± 0.003	111.99 ± 3.14
40	0.354 ± 0.002	0.058 ± 0.003	0.67 ± 0.08	0.376 ± 0.002	11.3 ± 0.15	0.526 ± 0.001	105.27 ± 1.31
45	0.180 ± 0.004	0.252 ± 0.011	2.55 ± 0.22	0.421 ± 0.009	16.18 ± 0.77	0.377 ± 0.009	91.33 ± 4.64

Observation time is 200 s.

for the blend containing 35 wt % TEC for a contact time longer than ~ 50 s are higher than for other blends. It is important to note that the dependence of adhesion parameters on contact time for the blend that contains 45 wt % TEC is less pronounced than that for blends with a lower plasticizer content. Indeed, the relaxation of the most liquid blend containing 45 wt % TEC occurs much faster than for other blends. The values of practical work of adhesion for the blend containing 45 wt % TEC are much lower than for the blends containing 30 or 35 wt % TEC (Fig. 24). On the other hand, the interpolymer complexes with lower plasticizer contents demonstrate solid-like behavior, with a highly pronounced maximum on the debonding curve and a low value of maximum elongation.

Figure 25 illustrates the general conclusion that can be derived from the analysis of this work. Large-scale relaxation processes within the polymer system, characterized by the values of the longer relaxation time (τ_3) predominantly govern pressure sensitive adhesion performance. This result confirms the prediction of eq. (6), which states that longer relaxation times are of particular importance for high adhesion. The best adhesion is observed for polyelectrolyte complex with longer relaxation times between 100 and 145 s. These values are appreciably longer than those obtained earlier for a range of commercial adhesives[37] that possess a somewhat higher adhesion at a comparable observation time of 200 s.

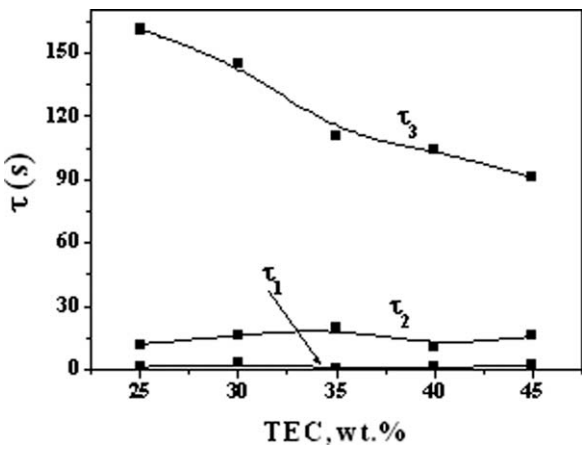

Figure 21 Relaxation times vs. TEC concentration in a polyacid–polybase interpolymer complex.

Water-absorbing capacity of PSA hydrogels based on nonstoichiometric polyelectrolyte complexes

Owing to formation of three-dimensional network of noncovalent intermacromolecular bonds, the PSAs based on nonstoichiometric ladder-like polyelectrolyte complexes are partially water insoluble, swelling rubber-like gels, which are capable to absorb great amounts of the water. As illustrated by the data in Figure 26, the polyelectrolyte complex formation leads to a loss in solubility of the polymer blend in water, expressed in terms of sol fraction (S), and a reduction of swell ratio (α), defined as the weight of the material in a swollen state divided by the dry weight of its gel fraction. The swell ratio is a fundamental characteristic of cross-linked polymeric gels that relates to the density of network junctions. The higher the density of the ladder-like network, the lower the swell ratio value.[67] The increase in LLC concentration (i.e., the decrease in FFP : LLC ratio) makes the ladder-like network denser and significantly decreases both the solubility (Sol Fraction)

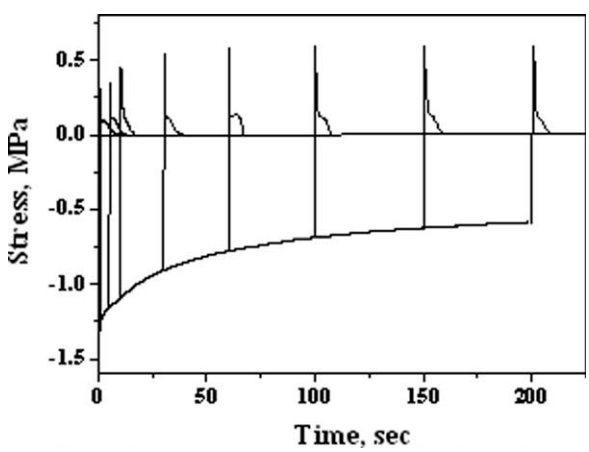

Figure 22 Effect of contact time on the curves of bonding stress relaxation, followed by probe separation from adhesive film surface under detaching force for interpolymer polybase–polyacid complex containing 35 wt % TEC.

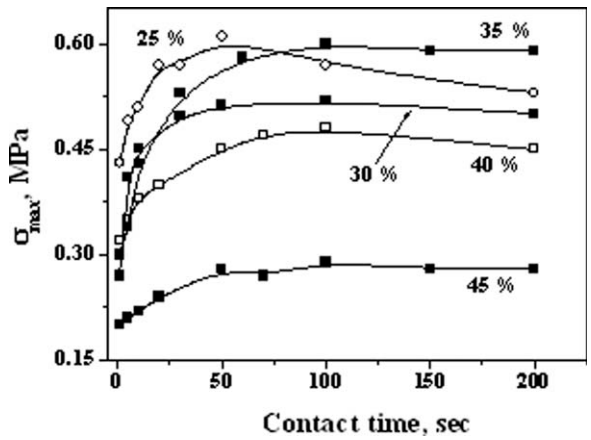

Figure 23 Effect of contact time on the maximum values of probe detaching stress (σ_{max}) for a plasticized interpolymer polybase–polyacid complex.

and the swelling of the researched interpolymer complex. As Figure 27 illustrates, the density of cross-links, expressed in terms of the swell ratio, controls the solubility of the ladder-like interpolymer complex. The reduction of both values is more pronounced at comparatively small LLC concentrations (below 40 wt %) (Fig. 26). Further increase in LLC content has only a negligible effect on dissolution and swelling properties

The swell ratio and the content of soluble fraction in the ladder-like nonstoichiometric complex of PDMAEMA-*co*-MMA/BMA with PMAA-*co*-EA depend on plasticizer concentration (Fig. 28). And also, the higher the hydrophilicity of the plasticizer, the greater the sol fraction and swell ratio values of the blends (Fig. 29). The 10% ionization of PDMAEMA-*co*-MMA/BMA and PMAA-*co*-EA polymers increases their solubility in water (Fig. 30). This behavior is also typical for their ladder-like nonstoichiometric complex containing 25 wt % TEC that exhibits a solid-like mechanism of debonding in

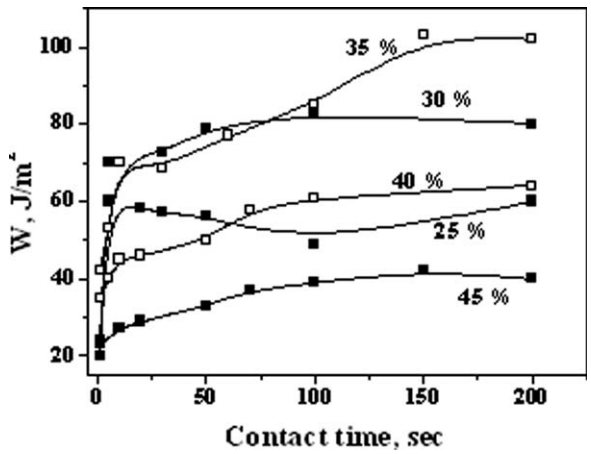

Figure 24 Effect of contact time on the practical work of adhesion (*W*) for the plasticized polyelectrolyte complex.

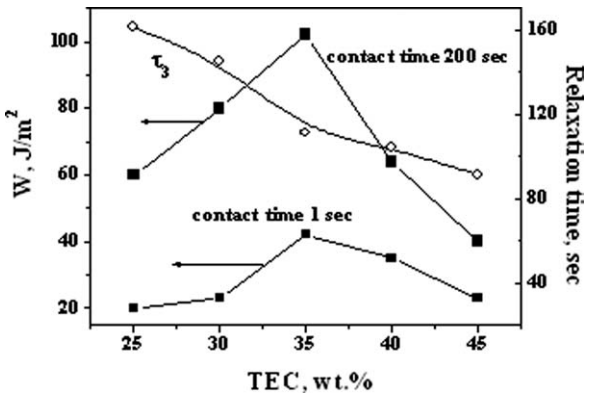

Figure 25 Effect of TEC content on the values of longer relaxation time (τ_3) and practical work of adhesion (*W*) for the PSA based on polyelectrolyte complex.

a Probe Tack test (Fig. 8). However, the blend with 35 wt % TEC, which reveals transitional probe tack profile from solid-like to fibrillar type of adhesive bond failure, demonstrates decreased solubility with 10% ionization of amino groups and an insignificant effect with the ionization of carboxyl groups (Fig. 30). In full agreement with the established mechanism of FFP–LLC interaction (see section The Energies of Intermolecular Bonds in Polybase–Polyacid Blends with and Without Plasticizer), 10% ionization of amino groups in FFP causes the drop in swell ratio, whereas the ionization of carboxyl groups of the LLC does not contribute to the swell ratio value or to the density of the interpolymer network (Fig. 31). For the complex containing 25 wt % plasticizer, no effect of 10% ionization of amino and carboxyl groups on the swell ratio value has been observed.

Replacement of PMAA-*co*-EA for more hydrophilic copolymer of maleic acid with methylvinyl ether (PMA-*co*-MVE) increases dramatically both the swell ratio (Fig. 32) and the sol fraction of their blends with PDMAEMA-*co*-MMA/BMA. The content of soluble fraction in this case is 88 and 49% for

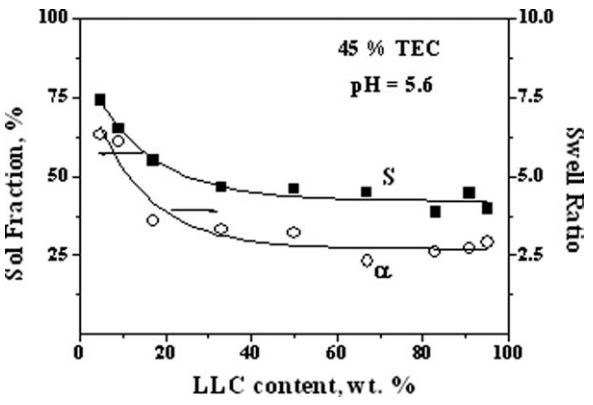

Figure 26 Effect of LLC concentration on sol fraction (*S*) and swelling ratio (α) of polyelectrolyte complex with 45 wt % TEC in water; pH 5.6.

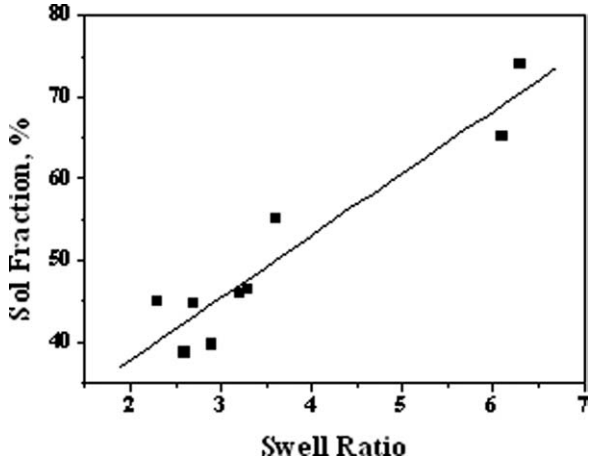

Figure 27 The content of the soluble fraction in the polyelectrolyte complex as a function of the value of swell ratio; pH 5.6. The plasticizer concentration was 45 wt %.

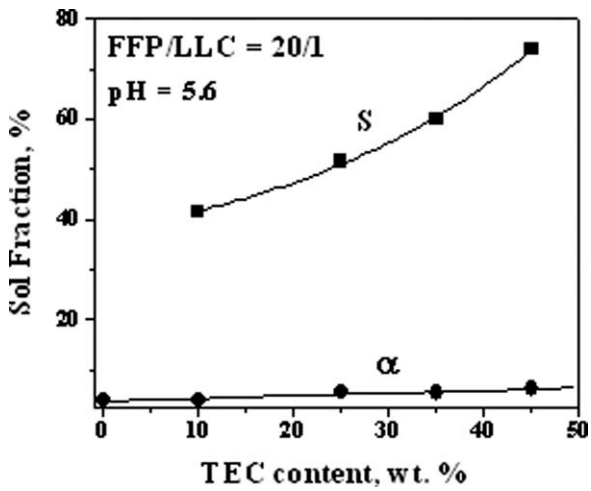

Figure 28 Effect of plasticizer concentration on solubility and water-sorbing capacity of the polyelectrolyte complex (FFP:LLC = 20 : 1).

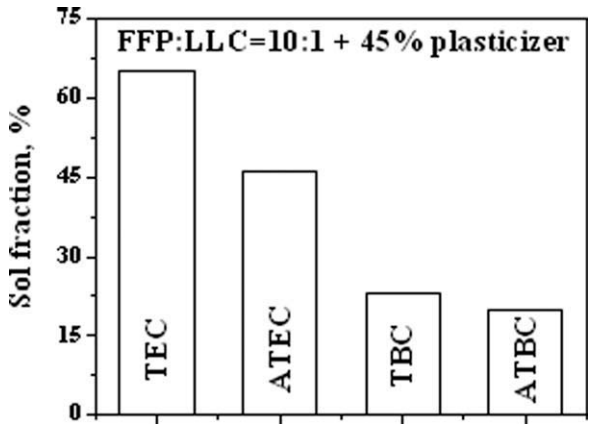

Figure 29 Effect of plasticizer hydrophilicity on the dissolution of considered polymer blends in water; pH 5.6.

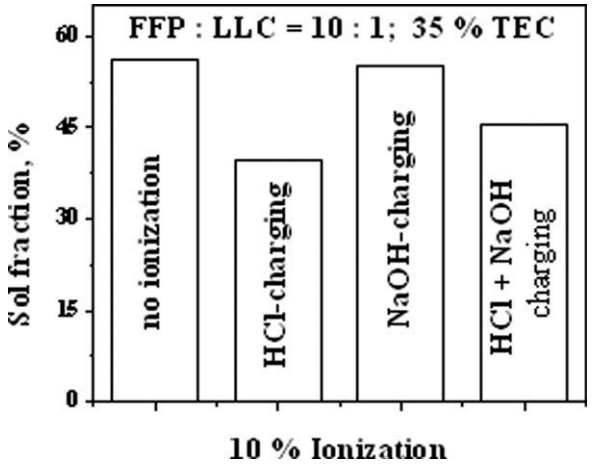

Figure 30 Sol fraction of plasticized interpolymer complex at 10% ionization of amino and carboxyl groups (FFP:LLC= 10 : 1); pH 5.6.

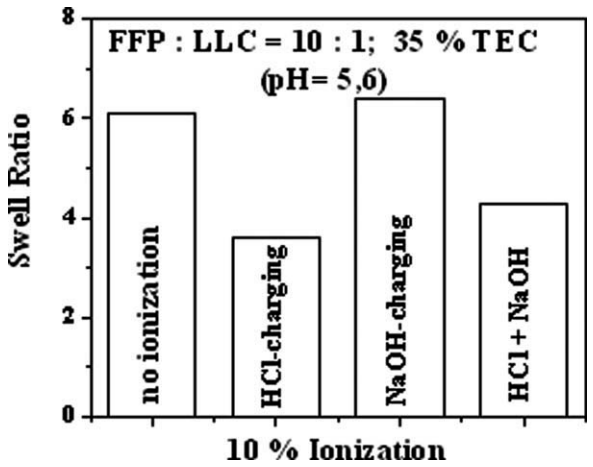

Figure 31 Swell ratio of plasticized polyelectrolyte complex with at 10% ionization of the amino (in FFP) and carboxyl (in LLC) groups.

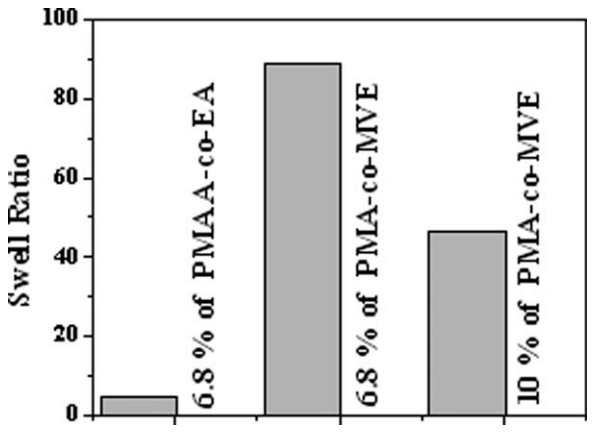

Figure 32 Swell ratio of PDMAEMA-*co*-MMA/BMA blends with different ladder-like crosslinkers: PMAA-*co*-EA and PMA-*co*-MVE.

the complexes with 6.8 and 10 wt % PMA-*co*-MVE, respectively.

In this way, the adhesive, mechanical and water-absorbing properties of polyelectrolyte blends can be easily manipulated by changing the relative composition of various copolymers in the blends and the ionization of their functional groups. Coupling adhesive properties with high water-absorbing capacity, typical for hydrogels, characterize the polyelectrolyte PSAs as innovative class of polymer composites with unique combination of performance properties. Owing to the presence of polar (ionic) and nonpolar groups in the copolymers, the materials based on polyelectrolyte complexes may be classified as "amphiphilic" adhesives. Such adhesives are compatible with both hydrophilic and hydrophobic substances and can be developed for diverse applications in various fields of industry, particularly in pharmacy for controlled drug delivery.

CONCLUSIONS

In this article, we have investigated the fundamental relationship linking molecular interaction mechanisms with nanostructure, phase behaviour and, finally, with a variety of unique physical properties of adhesive polyelectrolyte blends that absorb water and become, essentially, water-absorbing rubber-like adhesive hydrogel materials. Favorable properties such as ability to swell but yet retain both cohesiveness and tack, combined with processability, suggest a wide range of application of these materials, not only in industry but particularly in the biomedical and cosmetic fields. Bridging the gap between nanostructure and macroscopic physical properties of the polymer composites, based on nonstoichiometric polyelectrolyte complexes, along with gained molecular insight into macroscopic physical properties, allowed us to establish the function of every component in blend, and to lay the foundations for molecular design of innovative adhesive materials with tailored performance properties.

Notwithstanding the fact that chemical composition of the polyelectrolyte complex PSAs has nothing to do with the composition of typical PSAs, the adhesion behavior of these innovative PSAs obeys the same general lows, which are established for classical PSAs. The innovative PSAs based on polyelectrolyte and interpolymer hydrogen-bonded or electrostatic-bonded complexes can be easily produced by mixing complementary functional polymers in a common solution or in a melt state. Tackiness of initial polymer components is not obligatory condition for the production of adhesive composites. Taking into account many hundreds of functional homopolymers and copolymers, which are suitable to serve as the components of innovative PSA composites, the approach described in this article lays the foundation for the new area of the industry of adhesive polymer materials.

The PSAs based on ionic polyelectrolyte complexes represent an example of "smart," pH-responsive adhesive materials. They can be employed in various areas of industry and in medicine as electroconductive adhesives. New generation of the PSAs, described in this paper, opens numerous ways to the development of a wide variety of highly promising innovative industrial and pharmaceutical products on their basis.

The authors are thankful to Dr. M.B. Novikov, Mr. G.A. Shandryuk, and B.E. Gdalin for a range of measurements.

References

1. Van Krevelen, D. W. Properties of Polymers, 3rd ed., Elsevier: Amsterdam, 1990.
2. Askadskii, A. A. Physical Properties of Polymers: Prediction and Control; Gordon and Breach: Amsterdam, 1996.
3. Bicerano, J. Prediction of Polymer Properties: Marcel Dekker; New York, 1996.
4. Karelson, M. Molecular Descriptors in QSAR/QSPR; Wiley-Interscience: New York, 2000.
5. Todeshini, R.; Consonni, V. Handbook of Molecular Descriptors; Wiley-VCH: Weinheim, 2000.
6. Sun, H.; Tang, Y.; Zhang, F.; Wu, G.; Chan, S.-K. J Polym Sci Part B: Polym Phys 2002, 40, 2164.
7. Yu, X.; Wang, X.; Li, X.; Gao, J.; Wang, H. J Polym Sci Part B Polym Phys 2006, 44, 409.
8. Sun, H.; Tang, Y.; Wu, G.; Zhang, F. J Polym Sci Part B Polym Phys 2002, 40, 454.
9. Belfiore, L. A.; Lutz, T. J.; Cheng, C.; Bronnimann, C. E. J Polym Sci Part B Polym Phys 1990, 28, 1261.
10. Seitz, J. T. J Appl Polym Sci 1993, 49, 1331.
11. Gao, J.; Xu, J.; Chen, B.; Zhang, Q. J Mol Model 2007, 13, 573.
12. Kuhn, R.; Kroemer, H. Macrochim Acta 1991, 104(1–6), 225.
13. Andrews, E. H. Angew Chem 1974, 13, 113.
14. Klun, T. P.; Wendling, L. A.; Van Borgart, J. W. C.; Robbins, A. F. J Polym Sci Part A: Polym Chem 1987, 25, 87.
15. Grigorieva, O.; Slisenko, O.; Bismarck, A.; Sergeeva, L. Macromol Symp 2007, 254, 233.
16. Des Gennes, P. G. Introduction to Polymer Dynamics; Cambridge University Press, 1990.
17. Doi, M.; Edwards, S. F. The Theory of Polymer Dynamics; Oxford University Publishing, Oxford, New York, 1981.
18. Rohn, C. Analytical Polymer Rheology: Structure, Processing, Property Relationships; Hanser Publishing: New York, 1995, p 328.
19. Kinloch, A. J. Adhesion and Adhesives: Science and Technology; Chapman & Hall, London, 1987, Chapter 3.
20. Dillard, D. A.; Pocius, A. V., Eds., The Mechanics of Adhesion; Elsevier: New York, 2002.
21. Benedek, I.; Feldstein, M. M., Eds.; Handbook of Pressure-Sensitive Adhesives and Products; CRC/Taylor & Francis: London, 2009; Vols. 1–3.
22. Feldstein, M. M. In Handbook of Pressure-Sensitive Adhesives and Products, Fundamentals of Pressure Sensitivity; Benedek, I.; Feldstein, M. M., Eds., CRC/Taylor & Francis, London, 2009; Chapter 10, p 1.
23. Derail, C.; Marin, G. In Handbook of Pressure-Sensitive Adhesives and Products, Fundamentals of Pressure Sensitivity; Benedek, I.; Feldstein, M. M., Eds., CRC/Taylor & Francis, London, 2009; Chapter 4, p 1.

24. Chang, E.-P. In Handbook of Pressure-Sensitive Adhesives and Products, Fundamentals of Pressure Sensitivity; Benedek, I.; Feldstein, M. M., Eds., CRC/Taylor & Francis: London, New York, 2009; Chapter 5, p 1.
25. Kim, H.-J.; Lim, G.-H.; Park, Y.-J. In Handbook of Pressure-Sensitive Adhesives and Products, Fundamentals of Pressure Sensitivity; Benedek, I.; Feldstein, M. M., Eds; CRC/Taylor & Francis: London, New York, 2009; Chapter 7, p 1.
26. Lakrout, H.; Sergot, P.; Creton, C. J Adhesion 1999, 69 (3/4), 307.
27. Creton, C.; Shull, K. R. In Handbook of Pressure-Sensitive Adhesives and Products, Fundamentals of Pressure Sensitivity; Benedek, I.; Feldstein, M. M., Eds.; CRC/Taylor & Francis: London, New York, 2009; Chapter 6, p 1.
28. Yamaguchi, T.; Doi, M. Eur Phys J 2006, E 21, 331.
29. Kaelble, D. H. In Handbook of Pressure-Sensitive Adhesive Technology, 3rd ed.; Satas, D., Ed.; Satas & Associates: Warwick R.I., 1999; Chapter 6.
30. Ward I. M., Ed.; Mechanical Properties of Solid Polymers; Wiley Interscience: London, 1983; Chapter 2.
31. Voyutskii, S. S., Ed.; Autohesion and Adhesion of High Polymers; Wiley Interscience: New York, 1963.
32. Fujita H., Ed.; Diffusion in Polymer-Diluent Systems; Fortsch Hochpolym Forsch, 1961; p 1.
33. Novikov, M. B.; Borodulina, T. A.; Kotomin, S. V.; Kulichikhin, V. G.; Feldstein, M. M. J Adhesion 2005, 81, 77.
34. Novikov, M. B.; Gdalin, B. E.; Anosova, J. V.; Feldstein, M. M. J Adhesion 2008, 84, 164.
35. Feldstein, M. M. Polym Sci Ser A 2009, 51 (11–12), 1341.
36. Feldstein, M. M.; Novikov, M. B.; Creton, C. In Handbook of Pressure-Sensitive Adhesives and Products; Fundamentals of Pressure Sensitivity; Benedek, I.; Feldstein, M. M., Eds.; CRC/Taylor & Francis: London, New York, 2009; Chapter 11, p 1.
37. Feldstein, M. M.; Cleary, G. W.; Singh, P. In Handbook of Pressure-Sensitive Adhesives and Products; Technology of Pressure-Sensitive Adhesives and Products; Benedek, I.; Feldstein, M. M., Eds.; CRC/Taylor & Francis: London, New York, 2009; Chapter 7, p 1.
38. Feldstein, M. M.; Kireeva, P. E.; Kiseleva, T. I.; Gdalin, B. E.; Novikov, M. B.; Anosova, Y. V.; Shandryuk, G. A.; Singh, P.; Cleary, G. W. Polym Sci Ser A 2009, 51, 799.
39. Bayramov, D. F.; Singh, P.; Cleary, G. W.; Siegel, R. A.; Chalykh, A. E.; Feldstein, M. M. Polym Int 2008, 57, 785.
40. Kireeva, P. E.; Shandryuk, G. A.; Kostina, J. V.; Bondarenko, G. N.; Singh, P.; Cleary, G. W.; Feldstein, M. M. J Appl Polym Sci 2007, 105, 3017.
41. Kireeva, P. E.; Novikov, M. B.; Singh, P.; Cleary, G. W.; Feldstein, M. M. J Adhesion Sci Technol 2007, 21, 531.
42. Feldstein, M. M.; Bermesheva, E. V.; Jean, Y. C.; Misra, G. P.; Siegel, R. A. J Appl Polym Sci 2011, 119, 2408.
43. Dubin, P.; Bock, J.; Davis, R.; Schulz, D.; Thies, C., Eds. Macromolecular Complexes in Chemistry and Biology; Springer: New York, 1994.
44. Coleman, M. M.; Graf, J. F.; Painter, P. C. Specific Interactions and the Miscibility of Polymer Blends, Technomic Publishing: Lancaster, Basel, 1991.
45. Tsuchida, E.; Abe, K. Interaction Between Macromolecules in Solution and Intermacromolecular Complexes; Springer-Verlag: Berlin, 1982.
46. Kabanov, V. A.; Zezin, A. B. Pure Appl Chem 1984, 65, 343.
47. Jiang, M.; Li, M.; Xiang, M.; Zhou, H. Adv Polym Sci 1999, 146, 121.
48. Mende, M.; Petzold, G.; Buchhammer, H.-M. Colloid Polym Sci 2002, 280, 342.
49. Zhang, G.; Jiang, M.; Zhu, L.; Wu, C. Polymer 2001, 42, 151.
50. Izumrudov, V. A.; Sybachin, A. V. Polym Sci Ser A 2006, 48, 1098.
51. Kunze, K. K.; Netz, R. R. Europhys Lett 2002, 58, 299.
52. Philippova, O. E.; Khokhlov, A. R. In Polymer Gels and Networks; Osada, Y.; Kokhlov, A. R., Eds.; Marcel Dekker: New York, 2001; Chapter 7, p 163.
53. Zezin, A. B.; Rogacheva, V. B. In Advances in Physics and Chemistry of Polymers; Berlin, A. A.; Kabanov, V. A.; Rogovin, Z. A.; Slonimskii, G. L.; Khimiya, Eds.; Moscow: Khimiya (Chemistry in Russian), 1973; p 3.
54. Feldstein, M. M.; Kiseleva, T. I.; Bondarenko, G. N.; Kostina, J. V.; Singh, P.; Cleary, G. W. J Appl Polym Sci 2009, 112, 1142.
55. Kiseleva, T. I.; Shandryuk, G. A.; Khasbiullin, R. R.; Shcherbina, A. A.; Chalykh, A. E.; Feldstein, M. M. J Appl Polym Sci 2011, 122, 2926.
56. Raetzke, K. Personal communication.
57. Novikov, M. B.; Roos, A.; Creton, C.; Feldstein, M. M. Polymer 2003, 44, 3559.
58. Foresman, J. B.; Frisch, A. E. Exploring Chemistry with Electronic Structure Methods, 2nd ed.; Gaussian: Pittsburgh, 1996.
59. Gdalin, B. E.; Bermesheva, E. V.; Shandryuk, G. A.; Feldstein, M. M. J Adhesion 2011, 87, 111.
60. Michaels, A. S. Ind Eng Chem 1965, 57, 32.
61. Kabanov, V. A. Russian Rev Chem 2005, 74, 3.
62. Dahlquist, C. A. Adhes Age 1959, 2, 25.
63. Chalykh, A. A.; Chalykh, A. E.; Novikov, M. B.; Feldstein, M. M. J Adhesion 2002, 78, 667.
64. Poivet, S.; Nallet, F.; Gay, C.; Fabre, P. Europhys Lett 2003, 62, 244.
65. Déplace, F.; Carelli, C.; Mariot, S.; Retsos, H.; Chateauminois, A.; Ouzineb, K.; Creton, C. J Adhesion 2009, 85, 18.
66. Lindner, A.; Maevis, T.; Brummer, R.; Lűhmann, B.; Creton, C. Langmuir 2004, 20, 9156.
67. Cutié, S. C.; Smith, P. B.; Reim, R. E.; Graham, A. T. In Modern Superabsorbent Polymer Technology; Buchholz, F. L.; Garaham, A. T., Eds.; Wiley-VCH: New York, 1998; Chapter 4.